Fu and Mo *Nanoscale Research Letters* (2018) 13:187
https://doi.org/10.1186/s11671-018-2597-z

Nanoscale Research Letters

NANO REVIEW Open Access

A Review on the Electrochemically Self-organized Titania Nanotube Arrays: Synthesis, Modifications, and Biomedical Applications

Yu Fu and Anchun Mo*

Abstract

Titania nanotubes grown by anodic oxidation have intrigued the material science community by its many unique and potential properties, and the synthesis of technology is merging to its mature stage. The present review will focus on TiO_2 nanotubes grown by self-organized electrochemical anodization from Ti metal substrate, which critically highlights the synthesis of this type of self-organized titania nanotube layers and the means to influence the size, shape, the degree of order, and crystallized phases via adjusting the anodization parameters and the subsequent thermal annealing. The relationship between dimensions and properties of the anodic TiO_2 nanotube arrays will be presented. The latest progress and significance of the research on formation mechanism of anodic TiO_2 nanotubes are briefly discussed. Besides, we will show the most promising applications reported recently in biomedical directions and modifications carried out by doping, surface modification, and thermal annealing toward improving the properties of anodically formed TiO_2 nanotubes. At last, some unsolved issues and possible future directions of this field are indicated.

Keywords: Titania nanotubes, Biomedicine, Electrochemical anodization, Modifications

Introduction

Since the beginning of the twentieth century, titanium dioxide (TiO_2) has been used as commercial production in sun-blockers, paints, sensors, photocatalysis, solar cells, electrochromic devices, drug delivery, etc. [1–7]. The phenomenon that TiO_2 can produce the photogenerated electron-hole pairs under lighting irradiation can help split water into oxygen and hydrogen, benefiting to solve the energy crisis in the future as the most potential fuel. Fujishima and his co-workers first reported the photocatalytic water splitting on a TiO_2 electrode under ultraviolet (UV) light [8–10], and since then, titanium dioxide has become one of the most studied compounds in material science. Among all transition metal oxides, it presents a broad range of functional properties like chemical inertness, corrosion-resistance, and stability, especially the improvement of biocompatibility [11], and electrical and optical properties [1]. Ever since Iijima discovered carbon nanotubes in 1991 [12], showing a unique combination between the shape and functionality, where properties can be influenced directly by the geometry, enormous efforts have been made in the field of nanotechnology basically in chemical, physical, and biomedical material science.

Although the most explored nanomaterial so far is still the carbon, another class of nanotubular materials, which are usually based on transition metal oxides, has attracted considerable interests over the past 20 years. The first effort to form anodized titania nanotubes was made by Assefpour-Dezfuly [13] who used alkaline peroxide treatment followed by electrochemical anodization in an electrolyte containing chromic acid. And since Zwilling et al. reported that they produced the first self-organized nanotube layers on Ti substrate by electrochemical anodization in chromic acid electrolytes containing fluorine ions in 1999, the field has expanded enormously quickly [14]. Over the past decade, more than 33,800 papers with a keyword of "titania nanotubes" have been published.

* Correspondence: moanchun@163.com
State Key Laboratory of Oral Diseases, Department of Implantology, West China Hospital of Stomatology, Sichuan University, Chengdu 610041, China

Figure 1 gives the total publication broken down per year in the field of TiO_2 nanotubes and makes a comparison among different synthetic methods in the period 2002–2017 which not just shows an exponential growth trend but apparently indicates that the self-organized anodic TiO_2 nanotube arrays get much attention with great potential and advantages. Lately, Lee et al. has given a comprehensive and up to date view in the field of anodic titania nanotubes which almost covered all aspects including growth, modifications, properties, and applications with a brief of different synthesis approaches [15]. Compared with other preparation methods like hydro/solvothermal [16–18] and template-assisted methods [19, 20], direct oxidation turns out to be a simple technique with strong operability in which way the desired controllable nanostructure via adjusting size, shape, and the degree of order can be grown by means of optimizing the oxidation parameters such as the applied potential, time, temperature, pH, and the composition of the electrolyte [15]. Owing to the particular geometry, the self-aligned oxide nanotube layers which have highly organized structure and surface-volume ratio are representing unique properties, such as a very high mechanical strength, and the large specific surface area, even providing electronic properties like high electron mobility rate or quantum confinement effects [15, 21]. Furthermore, electrochemical anodization is a low-cost process and not limited to titanium but also can be suitable for other transition metals Hf [22], Zr [23], Nb [24], Ta [25], V [26] or alloys TiAl [27], and TiZr [28]. The present review will still focus on TiO_2 nanotubes grown by self-organized electrochemical anodization from Ti metal substrate. Besides, we will emphasize the synthesis of this type of self-organized titania nanotube layers and the means to influence the size, shape, the degree of order, and crystallized phases via adjusting the anodization parameters and the subsequent thermal annealing, including four different generations differing from electrolytes species and the defined two-step anodization, etc. The relationship between dimensions and properties of the anodic TiO_2 nanotube arrays will be presented. The latest progress and significance of the research on formation mechanism of anodic TiO_2 nanotubes are briefly discussed. We will show the most promising applications reported recently in biomedical directions and modifications carried out by doping, surface modification, and thermal annealing toward improving the properties of anodically formed TiO_2 nanotubes. We also consider unsolved issues and possible future directions of this field. The main paragraph text follows directly on here.

Synthesis of TiO_2 Nanotube Arrays by Electrochemical Anodization

In recent years, while many various forms of nanostructured titanium dioxide including nanorods, nanoparticles, nanowires, and nanotubes have been successfully developed [29–31], nanotubes have attracted increasing interests for technological applications due to the unique self-assembled structure with a large interfacial area and convenient controlling of the size and shape, which can be applied to surface area-dependent applications as a better candidate. A number of excellent reviews [1, 2, 15, 32–34] are available for dealing with the features of TiO_2 nanomaterials categorized with different synthetic methods. The electrochemical anodization is proved to be one of the most effective methods to obtain the

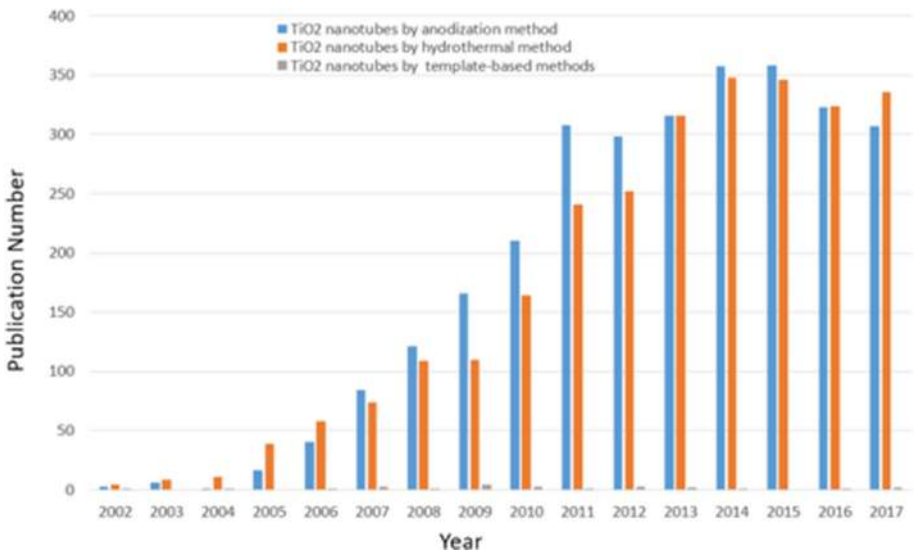

Fig. 1 Research trend. The number of papers broken down per year related to TiO_2 nanotubes differentiated by different synthesis methods from 2002 to 2017. (Data were collected from Science Citation Index Expanded using titania nanotubes, and anodization or hydrothermal methods or template-based methods as keywords)

titania nanotubes as a relatively simple technology that can be automated easily. We will specify the main techniques to fabricate anodic TiO_2 nanotubes below.

Self-organized Anodic TiO_2 Nanotube Arrays

As extensively studied, the titania nanotube layers can be formed under a specific set environmental conditions. The oxidation device consists of three parts: (I) a three-electrode system with the prepared Ti foil as the working electrode which is degreased by sequentially sonicating in acetone, ethanol, and deionized water, platinum as the counter electrode and usually Ag/AgCl as a reference electrode (Fig. 2a), while the pH electrode sometimes is added to obtain the ultimate concentration of F^- and HF [35] or another simple two-electrode system composed of Ti foil as anode and inert metal electrode as cathode (Fig. 2b) [36]; (II) generally, fluoride ion, chloride ion, chromium ion, bromide ion, or perchlorate containing electrolytes; and (III) a DC power supply. There are two main features influenced by the anodization conditions of formation affecting the promising applications of titania nanotubes: (I) geometry: size, shape, the degree of order, crystallized phases, etc. and (II) properties in chemical, physical, and biomedical. In other words, via controlling the electrochemical anodization parameters (applied potential, the duration of anodization, electrolyte system including the concentration of the fluorine ions, and water in the electrolyte, electrolyte temperature, electrolyte pH, etc. which will be discussed in more details in the "Synthesis of TiO2 Nanotube Arrays by Electrochemical Anodization" section), one can fabricate different titania nanostructures such as a flat compact oxide [1], a porous layer [1, 36], disordered TiO_2 nanotube layers growing in bundles [37], or finally a highly organized regular TiO_2

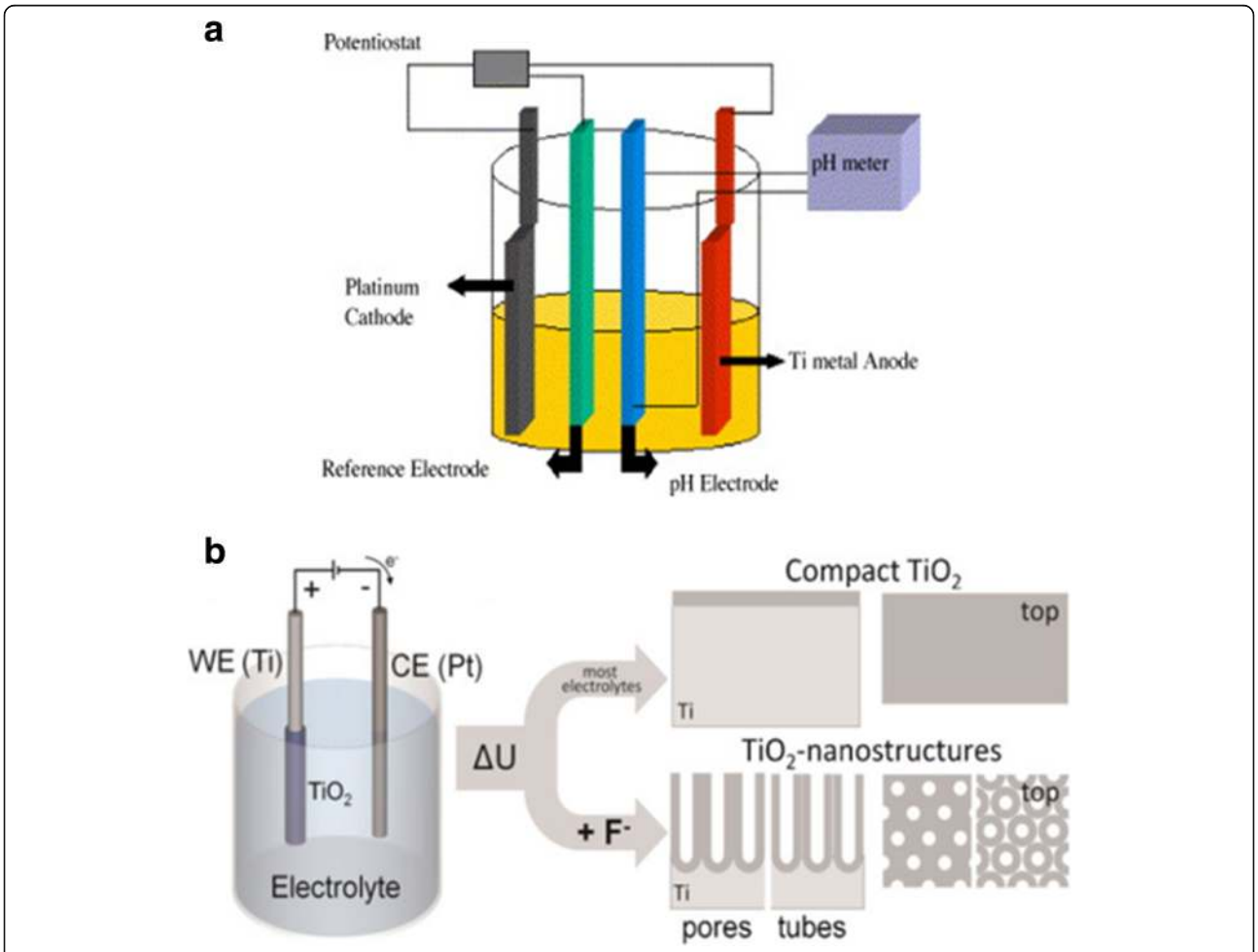

Fig. 2 Schematic set up. **a** Illustrative drawing of a three-electrode system with the prepared Ti foil as the working electrodes, platinum as the counter electrode, and usually Ag/AgCl as a reference electrode, while the pH electrode as a pH meter. Reproduced from ref. [35]. **b** Illustrative drawing of a simple two-electrode system composed of Ti foil as anode and inert metal electrode as cathode. Anodization leads to different anodized oxide layer under different conditions. In most neutral and acidic electrolytes, a compact titania can be formed. But if dilute fluoride electrolytes are used, nanotubular/nanoporous oxide layers will be directly attached to the metal surface. Reproduced from ref. [36]

nanotubes or advanced nanotubular layer: branched tube [38], bamboo-like [38, 39], double-walled [40], nanolace [38], or double-layer [39] structures in which way properties could be found differently. Figures 3 and 4 display field-emission scanning electron microscopy (FE-SEM) images of the typical examples of such TiO_2 nanotube morphologies.

(At present, TiO_2 nanotube arrays with tube diameters ranging from 10 to 500 nm, thickness of layers ranging from a few hundred nanometers to 1000 μm, and wall thickness ranging from 2 to 80 nm can be obtained [15, 41].)

It was two decades ago when Masuda and Fukuda for the first time reported the highly ordered porous alumina through adjusting the anodization conditions to an optimum [42]. Later on, researchers spent their efforts to make similarly organized structures also for TiO_2 nanotube layers. And there are three crucial factors affecting the degree of order in anodic TiO_2 nanotube arrays (in accordance with polygons in the layers and the standard deviation in tube diameter): the Ti substrate, the applied voltage, and the repetitive anodization [33, 43]. It is obvious that fewer flaws in the arrangement can be obtained for high purity material at the highest possible voltage below dielectric breakdown [33] and the ideally hexagonal self-ordered TiO_2 nanotubes as shown in Fig. 5 can be improved significantly by secondary tubes growth [43]. Sopha et al. showed impurities strongly influence the resulting different dimensions and ordering of nanotubes after the second anodization [44]. Moreover, the crystallographic orientations of the Ti substrate grains have been revealed to be crucial effects in growth characteristics of TiO_2 nanotube arrays by electron backscatter diffraction (EBSD). Leonardi et al. found that nanotubes can only be observed with an orientation that enables a valve metal oxide to form on grains allowing penetration of fluoride ions through the oxidation film where 1 M $(NH_4)H_2PO_3$+0.5 wt% NH_4F were used as electrolyte [45]. Similarly, Macak and co-workers reported that no nanotube growth on grains is retarded in the widely used ethylene glycol-based electrolyte compared to the case of using aqueous electrolyte, as known from the last literature [46]. On the polished Ti sheet, grains with [0 0 0 1] orientation or close to this turned out to be the ideal grains and utilizing single-crystalline Ti with ideal orientation would be a great advance to obtain the most uniform nanotube arrays [46].

Nevertheless, there are still some defects influencing the degree of order. Lately, it has been further extended by uniform nanoimprinting Ti. Kondo et al. figured out a throughput fabrication of an ideally ordered anodic TiO_2 by nanoimprinting Ti surface or a two-layered specimen with an Al layer on the top and the Ti layer at the bottom using a Ni mold with ordered convexes. And the

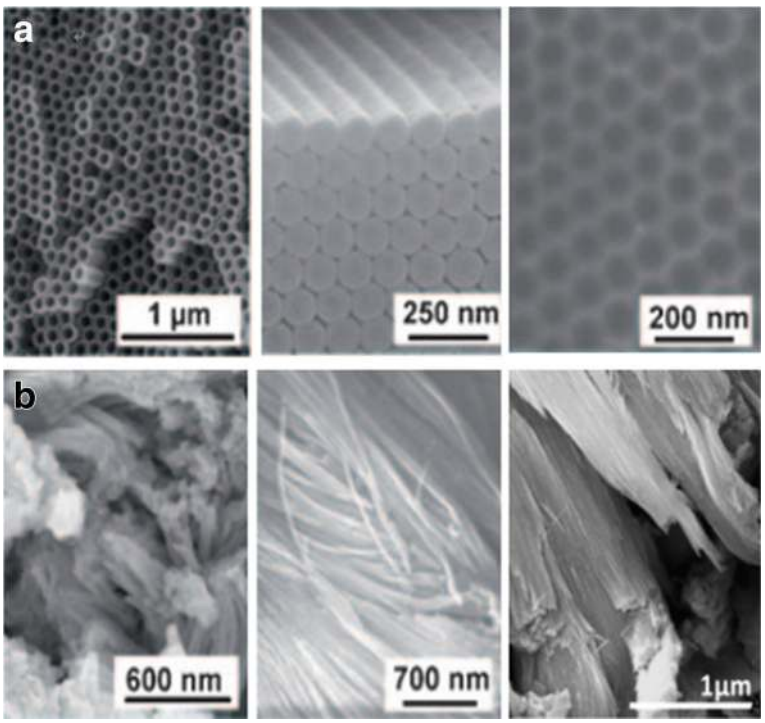

Fig. 3 SEM images of anodized TiO_2 nanotube layers by different anodization processes of Ti. **a** The highly ordered TiO_2 nanotubes (in top and side view) are obtained in organic electrolyte systems, with self-ordered surface dimples (right) which in fact are metallic surfaces when the tube layers are removed. Reproduced from ref. [1]. **b** The disordered TiO_2 nanotubes are grown in patches on the surface area and fused together to bundles in chloride containing electrolyte by an ultrafast anodization technique known as rapid-breakdown anodization (RBA). Reproduced from ref. [1] and [37]

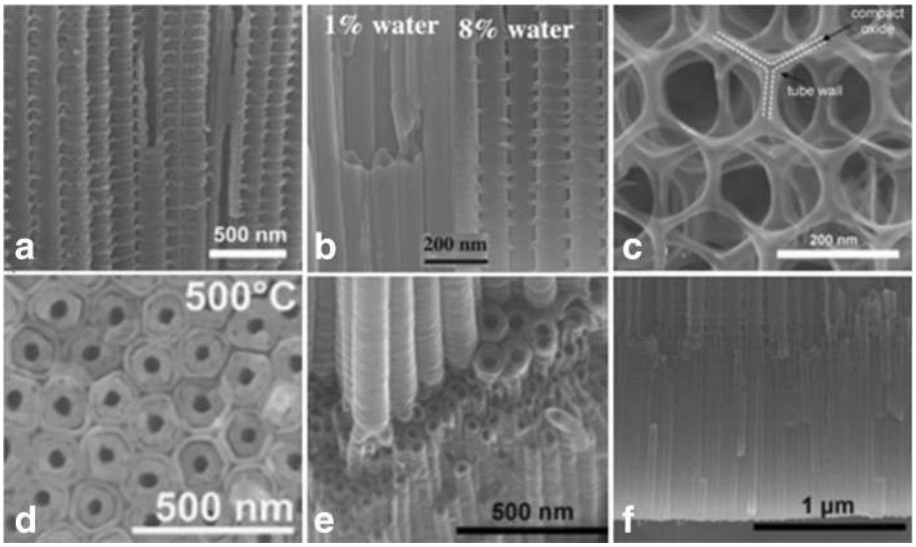

Fig. 4 SEM images of advanced TiO_2 nanotube morphologies. **a** Bamboo-type reinforced TiO_2 nanotubes are fabricated under specific alternating-voltage (AV) conditions in ethylene glycol consisting of 0.2 mol/L HF, with a sequence of 1 min at 120 V and 5 min at 40 V. Reproduced from ref. [38]. **b** Transition from smooth to bamboo-like TiO_2 nanotubes can be induced by anodization with controlled water addition (water contents:1 to 8%) to a 0.135 M NH_4F/ethylene glycol electrolytereproduced from ref. [39]. **c** The 2D nanolace structures are obtained under voltage cycling carried out for an extended period of time in the fluoride containing electrolyte, with a sequence of 50 s at 120 V and 600 s at 0 V. Reproduced from ref. [38]. **d** The double-walled TiO_2 nanotubes are grown by anodization of Ti in a fluoride containing ethylene glycol electrolyte at 120 V after annealing at 500 °C with a heating rate of 1 ° C s^{-1}. Reproduced from ref. [40]. **e** The branched nanotubes can be observed by voltage stepping, first at 120 V (6 h) and then at 40 V (2 h). Reproduced from ref. [38]. **f** The double-layer nanotubes with equal or two different tube diameters can be seen. Reproduced from ref. [38]

TiO_2 layers could be generated in a more orderly way where the shallow concaves of the pre-textured pattern acted as initiation sites by the subsequent anodization in NH_4F ethylene glycol solution [47, 48]. Following closely, Sopha et al. firstly covered a TiN-protecting layer on Ti substrate prepared by atomic layer deposition (ALD) before the pre-texturing carried out by focused ion beam (FIB) and the subsequent anodization using ethylene glycol electrolyte to produce perfectly hexagonally arranged nanotube layers with a thickness of 2 μm, which can restrict the nanotubes only to grow on the given initiation sites and extend anodization time without any defects [49].

Formation Mechanism of Anodic TiO_2 Nanotubes

Anodic oxidation technology and researches on formation mechanism of anodic TiO_2 nanotubes has captured wide attention for a long time from a broad diversity of disciplines. The mechanism research Diggle reported in 1969 about the films of compact anodic oxide and porous anodic oxide [50] now still plays an extremely important guiding role. A significant amount of recent works show that transition from pores to tubes is of a gradual nature [1, 27, 36]; however, the fully theoretical model and reasoning were not given.

Conventional field-assisted dissolution (FAD) is the most acceptable theory [1, 33, 51]. That is in the process of electrochemical anodization, TiO_2 nanotube arrays are formed by self-organization of titania because of three relatively independent procedures: electrochemical oxidation of Ti into TiO_2, the electrical field-induced dissolution of TiO_2, and the fluorine ion-induced chemical dissolution of TiO_2, reaching a delicate balance. As a characteristic current time curve shown in Fig. 6 for electrolytes containing fluoride that lead to nanotube formation [51] and a typical image that can help to illustrate the formation process schematically [33] shown in Fig. 7, the transient can be divided into three distinct stages: (I) In the first part, there is a current decay, caused by a newly formed barrier oxide, when the two major processes, the inward migration of O^{2-} ions toward the metal/oxide interface and the outward migration of Ti^{4+} ions toward the oxide/electrolyte interface, achieve a balance. (II) In the second part, the current begins to rise again with a time lag caused by the increasing surface area of the anode. The shorter the lag is, the higher the fluoride concentration will be due to the fluoride-induced dissolution of the formed TiO_2, and pores start to fabricate randomly which subsequently turn out to be the initial formation of TiO_2 nanotubes. (III) Then, the current reaches a steady state, when the pore growth rate at the metal oxide interface and induced dissolution rate of the formed TiO_2 at the outer interface reach an equilibrium situation. Thus, the final tubes become increasingly v-shaped, that is, the tops of the tubes possess significantly thinner walls than their bottoms where the tubes are closed-packed. The gradient in the tube wall thickness in Fig. 5 can be ascribed

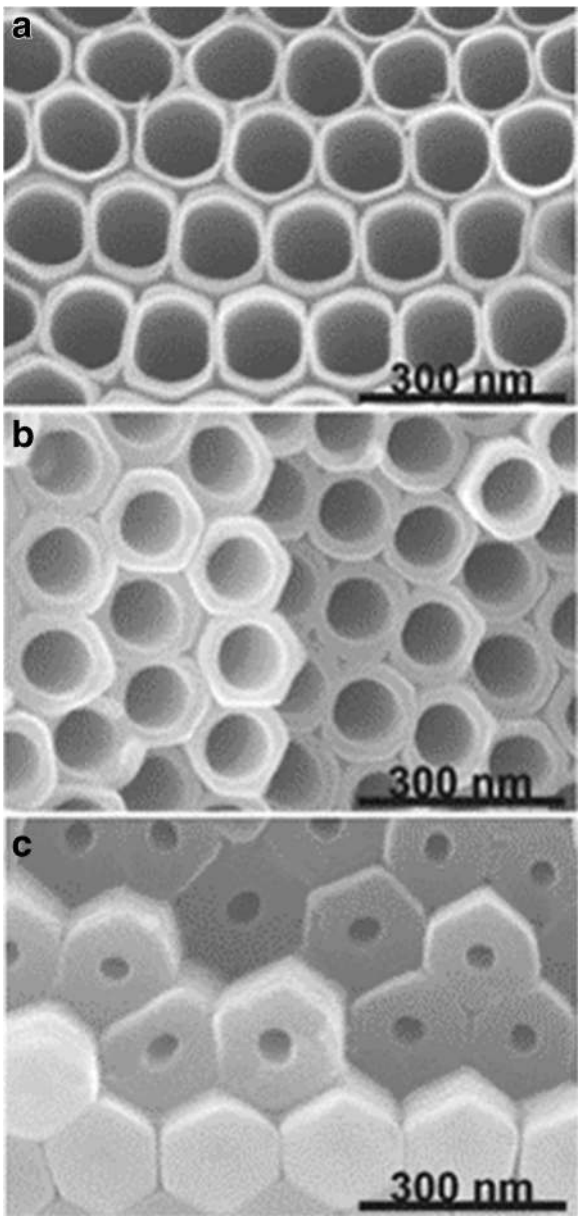

Fig. 5 SEM images of TiO_2 nanotubes. The nanotubes are formed in ethylene glycol electrolytes containing 0.27 M NH_4F by repeated anodization of Ti. The cross sections are taken at the top of the layer, in the middle, and at the bottom of the layer. Reproduced from ref. [43]

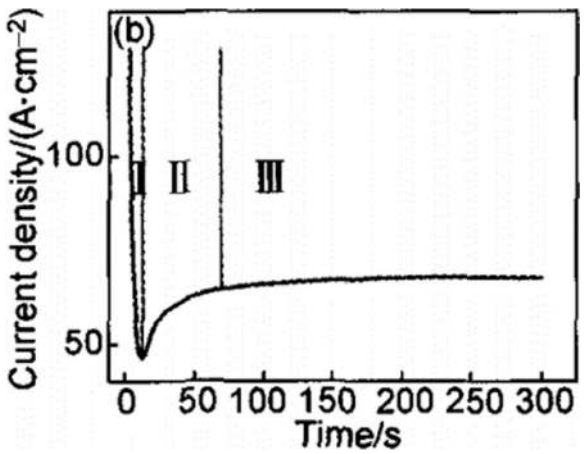

Fig. 6 Typical current time curve under a constant voltage in electrolytes containing fluoride. The transient can be divided into three distinct regions (**I**–**III**). (**I**) In the first part, there is a sharp current decay. (**II**) In the second part, the current begins to rise again with a time lag. (**III**) In the third part, the current reaches a steady state reproduced from ref. [51]

to different exposure time and concentration to the electrolytes along the tubes [43].

However, this theory cannot explain the phenomenon of separation into tubes, as opposed to a nanoporous structure clearly yet, and Fahim et al. observed that under appropriate voltages it is possible to obtain titania nanotubes in sulfuric acid solution without fluoride ions, in which case, the I-t curve resembled the one we just discussed above [52]. As Houser and Hebert pointed out, growth mechanism have not yet been developed to explain the quantitative relationships between the process of titania porous membrane and I-t curve [53]. Because the interpretation is not convincing enough, new points about the mechanism appear recently such as viscous flow model and growth model of two currents. With regard to these mechanisms, a review [51] shows lots of limitations for the traditional field-assisted dissolution theory and makes some explanations on latest progress and significance of the research on viscous flow model and growth model of two currents.

The Effect of Anodization Conditions Affecting Geometry and Properties

The composition and concentration of the electrolytes have significant influence in the nanotube arrays formation. According to the difference of electrolytes we use, the development is basically divided into three stages: Table 1 summarizes the anodization conditions and dimensions of the resulting TiO_2 nanotube arrays in the three generations investigated by different research groups to date.

The first generation: hydrofluoric acid (HF)-based aqueous electrolytes

The milestone is that Gong et al. for the first time presented the uniform titania nanotube arrays by anodic oxidation of Ti in HF-based aqueous electrolytes [54]. In HF aqueous solution electrolytes, where pH is relatively low meaning high concentration of hydrogen ions, the chemical dissolution of TiO_2 induced by fluorine ions plays the dominant status in the anodization process [55]. A dynamic equilibrium was achieved in a short period of time in the process of forming titania nanotubes, and

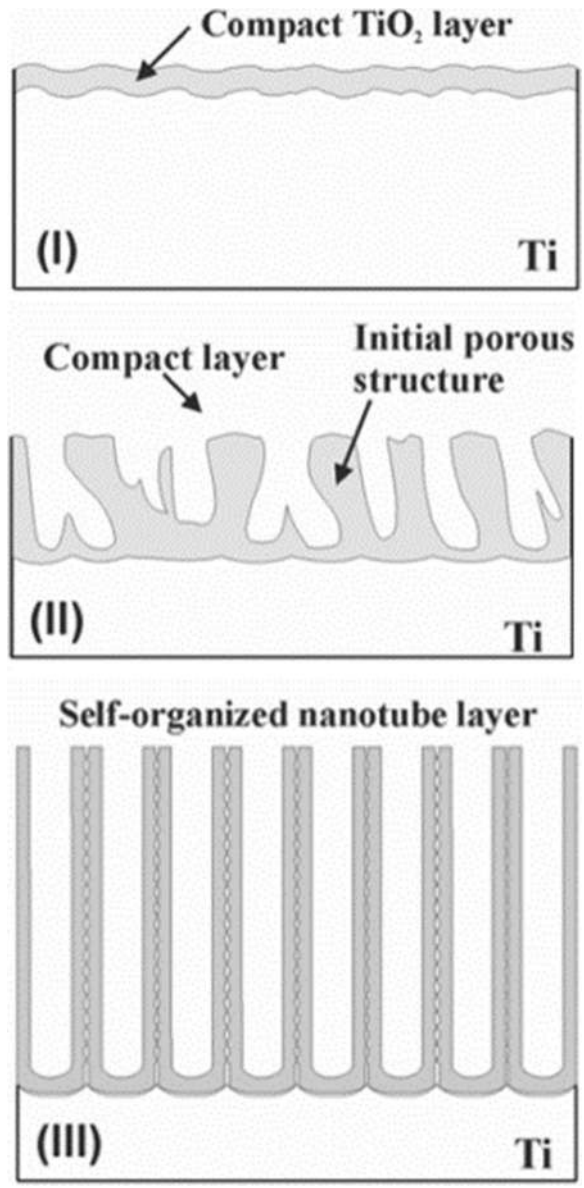

Fig. 7 The forming process of TiO_2 nanotube arrays. The formation of TiO_2 nanotube arrays can be divided into three different morphological stages (**I**–**III**). (**I**) A barrier oxide is formed. (**II**) The surface is locally activated and pores start to grow randomly. (**III**) Self-organized nanotube layer is formed reproduced from ref. [33]

therefore, the maximum achievable nanotubes length was restricted to approximately 0.5 μm [54–56].

The second generation: buffered electrolytes

In the subsequent work, in order to reduce chemical dissolution lengthening the tubes, Cai et al. demonstrated that by adding weaker acids such as KF or NaF into a buffered solution and adjusting the pH to weakly acidic (pH = 4.5) with sulfuric acid or sodium hydroxide, nanotubes approximately 4.4 μm in length were achieved [57]. PH value affects the hydrolyzation of the titanium ions which turn out to interfere the electrochemical etching and chemical dissolution. Cai et al. also pointed out that lower pH values produce shorter but clean nanotubes and higher pH values result in longer nanotubes but unwanted debris [57]. As the pH value goes up, the rate of hydrolysis will increase, in turn slowing down the chemical dissolution, leading to longer nanotubes while alkaline solution is not suitable for nanotubes growth [57, 58]. It is demonstrated that in neutral NaF electrolyte at proper voltage much longer nanotubes could be obtained than in acidic solutions by Macak et al. [58]. Given a particular voltage in fluoride containing electrolyte, by adjusting the pH gradient, the required aspect ratios and thickness of layers could be achieved [59].

The third generation: polar organic electrolytes

Electrolytes such as glycerol [59], dimethyl sulfoxide [60], formamide or diethylene glycol [61, 62], ethylene glycol [41, 63], containing fluoride species such as NH_4F, NaF, and KF gradually appear. Macak and co-workers took the lead in using viscous glycerol electrolyte to fabricate titania nanotube arrays with the thickness of approximately 7 μm and an average tube diameter of 40 nm [59]. It is demonstrated that higher aspect ratio TiO_2 nanotubes can be grown in such polar organic electrolyte due to proper control of electrolyte pH reducing chemical dissolution of the titania [64]. Paulose et al. formed nanotubes approximately 134 μm in length, prepared using ethylene glycol containing 0.25 wt% NH_4F at an anodization potential of 60 V for 17 h [60]. Soon afterwards, more than 250-μm-thick TiO_2 nanotube arrays were reported by Albu [65]. Besides, the water content plays a dual role in the process: it is indispensable for the formation of titania, but it also speeds up the chemical dissolution [63]. Hence, how to shrink the effect of water content to a minimal significance is required for increasing the thickness and degree of order of the TiO_2 nanotube arrays. In general, limiting water content to less than 5% is the key to achieve very long nanotubes successfully [60], and a minimum amount of water content (0.18 wt%) is required to form well-organized titania nanotubes [66]. It was reported that with the addition of water, the current density recorded decreased which was the highest in anhydrous ethylene glycol solution [66]. Paulose et al. first reported formation of self-organized hexagonally titania nanotube arrays with approximately 1000 μm in length at 60 V for 216 h in ethylene glycol containing 0.6 wt% NH_4F and 3.5% water [41]. Another noticeable phenomenon is that smooth tube walls are grown at low water content, while ripples on side walls are formed at higher content as shown in Fig. 4b [59, 67]. As by far the most employed type of electrolytes, ethylene glycol containing water and fluoride ions always leads to a double-walled nanotube structures (Fig. 4d) [40, 68–70], while the inner layer can be removed by a suitable annealing treatment followed

Table 1 TiO_2 nanotubes arrays fabricated through anodic oxidation in the three generations: electrolyte compositions, anodization conditions, and size of the resulting nanotubes

Generation	Electrolyte	Condition	Diameter	Thickness of layers	Ref
First generation	0.5 wt% HF in aqueous solution	20 V 20 min	60 nm	250 nm	[54]
second generation	0.1MKF+1MH_2SO_4+0.2Mcitric acid	25 V 20 h	115 nm (inner)	4.4 μm	[57]
	1MNa_2SO_4+0.5wt%NaF	20 V 6 h	100 nm	2.4 μm	[58]
Third generation	0.5 wt% NH_4F	20 V	40 nm	7 μm	[59]
	In glycerol	13 h			
	0.3 wt% NH_4F	60 V	100 nm	45 μm	[63]
	In ethylene glycol	18 h			
	0.25 wt% NH_4F	60 V	160 nm	134 μm	[60]
	In ethylene glycol	17 h			

by a simple chemical etching process. After removal of the inner shell, the widened tubes allow a layer-by-layer decoration with nanoparticles using a repetitive approach based on $TiCl_4$-hydrolysis [71]. Whereas single-walled tubes showed significantly enhanced conductivity and electron transport times in dye-sensitized solar cells (DSSCs) [71, 72] where the thickness of the entire tube is basically the same and the inner shell no longer appears, Mirabolghasemi et al. made a comparison between the double- and single-walled tubes and presented desired single-walled tubes with an addition of dimethyl sulfoxide (DMSO) into electrolytes with 1.5 M H_2O and 0.1 M NH_4F [72].

Recently, non-fluoride-based electrolytes have been reported to grow TiO_2 nanotube arrays which may be considered as the fourth synthesis generation including hydrochloric acid, hydrogen peroxide, perchloric acid solutions, and their mixtures [73, 74]. Allama and Grimes described well-developed nanotube arrays with 300 nm in length, 15 nm in inner diameter, and 25 nm in outer diameter were obtained in a 3 M hydrochloric acid (HCl) aqueous electrolyte at oxidation voltages between 10 and 13 V. But adding a low concentration of H_3PO_4 resulted to a change from nanotubes to rods. They further suggested that they were unable to achieve self-organized nanotube arrays in HCl-containing electrolytes at the concentration of lower or higher than 3 M [73]. Allama found out that adding hydrogen peroxide to the hydrochloric acid containing aqueous solution could be a possible method to lengthen the titania nanotubes which possesses a strong oxidizing property following a thicker oxide layer, demonstrating that fluoride ions can successfully be replaced by chloride ions in the growth of nanotube arrays [74]. Besides, ionic liquids without addition of free fluoride species have been treated as another type of solvent system for titania nanotubes in recent years [75, 76].

In addition to the standard parameters, the geometry of the resulting nanotubes is dependent on the repetitive use of electrolyte (the "used solution effect"). In comparison with the tubes obtained with fresh solutions, using once-used solutions, exhibited an increase in nanotube length and a better quality where the nanotube growth rate achieved is consistently higher for once-used solutions at 60 V and above [77] and a slightly different but distinguishable current transient behavior could be noted [66]. Moreover, no nanotubular structure but an oxide film was obtained in the twice-used solution because of the depletion of F^- species [78]. However, Sopha et al. investigated different ages of ethylene glycol based electrolytes on the morphology of TiO_2 nanotubes showing that in older electrolytes the arrays exhibit lower aspect ratios [79].

Applied Potential

Anodization voltage is the critical factor controlling tube diameters [80, 81]. The dimension of the nanotube arrays can be predicted just simply by applying the suitable range of voltage called potential window across the electrode [67]. At a low voltage, less electric field dissolution occurs, forming TiO_2 nanotubes with smaller diameters. If the voltage is too low, the TiO_2 layer becomes compact but no nanotubular structure can be observed. On the contrary, a spongy-like porous structure will be seen when the voltage is too high. With controllable voltage, the diameter of the nanotubes is proportional to the voltage [81]. Furthermore, studies show that the range of voltage forming nanotubes is also related to the electrolyte system. In aqueous electrolytes, the potential window should be controlled from 10 to 25 V, which in organic electrolytes is much wider between several volts and some hundred volts. Wang and Lin found out the fact that in aqueous electrolytes, the anodization potential exhibits significant influence on the growth of TiO_2 nanotube arrays, which exhibited slight influence in non-aqueous electrolytes in this regard [82]. The voltage dependence has a significant reduction in non-aqueous

electrolytes which is attributed to a large extent to the low conductivity of organic electrolytes [83, 84].

The Duration on Anodization

The duration of anodization affects the nanotubes mainly in two aspects: (I) the formation of the tubes or not and (II) the length of the tubes. That is, in the early stage of the anodization, a compact TiO_2 film is formed. If the duration is too short to reach an equilibrium in reaction, the regular nanotube array cannot be achieved instead of a disordered porous layer [67]. With increasing the anodization time, porous structure gradually grows deeper and converts into the TiO_2 nanotubular array [1, 33, 51]. If other electrochemical parameters are kept unchanged, increase in the nanotube length is observed over time while no significant effect on diameter and tube wall thickness until a steady-state situation occurs [67, 85, 86]. However, due to the decrease of the F^- concentration in the electrolyte, where the ion transport rate decreased, the growth rate of nanotubes is reduced. After reaching a stable condition between tube growth at the bottom and chemical/electrochemical dissolution at the top, we will find no further increase in length of the nanotubes [87]. As time continues to go, pipe orifice becomes an irregular polygon resulting in TiO_2 spikes and coverings which can be seen on the surface of the TiO_2 nanotube arrays [36]. It is worth mentioning that enlightened by the success of aluminum-repeated anodization for self-organized porous alumina [88], the two-step anodization of titanium for such a highly ordered hexagonally packed nanostructure of titania has appeared [43, 77, 89–91]. After the first-step anodization, the first nanotube layer from the Ti foil should be removed ultrasonically or by using an adhesion tape which leads to a surface where the remaining Ti is covered by comparably ordered dimples. Researches have shown that the former treatment helps to avoid potential mechanical damage to the Ti surface and also improve the structural uniformity of the TiO_2 nanotubes to a great extent [77, 90, 91]. In the second anodization step, the pretreated Ti foil would be used as anode again with or without changes in parameters of oxidation conditions. It is subsequently found that the highly ordered and vertically oriented titania nanotubes, have greater potential in such fields as photocatalysis [77], photoelectriochemical activity [92, 93], and biological interaction with cells [94] than the disordered nanotubular titania.

Electrolyte Temperature

Temperature restricts the growth and quality of titania nanotube arrays, directly affecting the rate of oxide growth, length, and wall thickness of the structure [64, 95]. Wang and Lin first reported the effect of electrolyte temperature in both aqueous and non-aqueous electrolyte on anodic oxidation of titanium [82]. In aqueous electrolyte, with the temperature increasing, a slight diminish in the internal diameters was observed while the external diameters remained the same [68]. The reason may be the dissolution induced by electrical field and fluoride ions are similar while the oxide formation rate is higher than that at lower temperature. In non-aqueous electrolyte containing fluoride ions, the outer nanotube diameter was found to be largely increased by the increasing electrolyte temperature [82]. This may be because at lower temperature, the ion mobility of fluorine in some viscous electrolyte is further inhibited, leading to much slower dissolution of newly formed titania, which subsequently lead to a smaller nanotube diameter. As chemical dissolution rate increases, surface of TiO_2 nanotubes arrays can easily produce excessive corrosion, resulting in lodging nanotubes and agglomeration. Therefore, the appropriate bath temperature for stable TiO_2 nanotube arrays is at room temperature [82, 95, 96].

Modification of Nanotubes Properties

Increasing applications of TiO_2 nanotubes as a novel semiconductor are closely related to its photoelectriochemical (PEC) performance; however, they are sometimes prevented by two fundamental drawbacks: (I) the wide band gap (3.0 eV for the rutile phase and 3.2 eV for the anatase phase) can only absorb ultraviolet light, which accounts for less than 10% of the sunlight [97], resulting in low average utilization ratio of solar energy and (II) the low electrical conductivity cannot efficiently transfer photogenerated carries. At the same time, the photoelectrons and vacancies can be easily recombined, thus making low electron mobility rate or quantum confinement effects [98]. Hence, post-treatment of TiO_2 nanotubes is the key to improve the performance of its materials and related devices successfully. Considerable researches have been reported on modified methods to reduce the recombination of photogenerated electron-hole pair rate, speed up the electron transfer rate, and enhance the photoelectriochemical activity of TiO_2 nanotubes. The research of the methods for the improvement of the photoelectriochemical properties of TiO_2 nanotubes will be reviewed, including thermal annealing, doping, and surface modification. As for promising modification in biomedical fields, we will present in the application section.

Thermal Annealing

The crystallinity of the nanotube arrays and their conductivity, lifetime of charge carrier, and photoresponse depend mainly on the thermal annealing temperature and atmosphere [99, 100]. The as-prepared TiO_2 nanotubes above are amorphous in nature but can be annealed to anatase or rutile phase, or mixtures of both phases relying on the specific temperature [1, 3, 40, 92,

100]. It is demonstrated that amorphous nanotube layers grown in a glycerol-based electrolyte containing fluoride ions have low photocurrents and an incident photon-to-electron conversion efficiency (IPCE) below 5% due to lots of structural defects while anatase phase nanotubes exhibit an IPCE value up to 60% thus attracting more interest to applications such as dye-sensitized or perovskite solar cells [93]. As well in mixed water-glycerol electrolyte with F^-, Das et al. stated their points that if the self-organized TiO_2 nanotube arrays with thickness about 1 μm were annealed around 300–500 °C, the anatase phase of TiO_2 as the most preferred crystalline structure could be observed. The single anatase structure of nanotubes with the best photoelectriochemical properties and the lowest resistivity could be fabricated when annealed at 400 °C. At temperature higher than 600 °C, a track of typical rutile appeared and with a further increase in annealing temperature the percentage and quality of the rutile phase increased [92]. It should be noted that in Jaroenworaluc's work, rutile phase was detected in anodic nanotube layers grown in aqueous NaF/Na_2SO_4 with thickness of approximately 1.5 μm at 500 °C heat treatment and became the dominant phase at 600 °C. Whereas at 550 °C, partial nanotubes began to break down [101]. It begins to cause the collapse of the entire nanostructure formed in aqueous NaF/Na_2SO_4 with the continuous increase of temperature (800–900 °C) or the extended annealing time [3]. While for extended temperature, the crystalline structure of the nanotubes completely converts to rutile phase at above 900 °C [3]. Some researchers demonstrated a loss of the typical single-walled nanotube layers morphology when the annealed temperature rose above 580 °C [102]. Besides the whole annealing process especially the heating rate controls, the morphological structures of the entire nanotube arrays [40]. The double-walled nanotube layers prepared from ethylene glycol (containing less than 0.2 wt% H_2O), with the addition of HF and H_2O_2, have such a high stability that can keep their structure intact until temperature is higher than 900 °C with a heating rate of 1 °C s^{-1}. However, the double-walled nanotubes begin to collapse as soon as the temperature reaches 500 °C when the heating rate is 25 °C s^{-1}. Most extraordinarily, with the high speed of 50 °C s^{-1} the entire separated nanotubes fuse into a highly ordered porous membrane [40]. Xiao et al. obtained crystallized titania nanotubes arrays with calcination in different gases like dry nitrogen, air, and argon indicating nanotubes in dry nitrogen appeared to have enhanced electrochemical and photoelectrical properties who also found out that with the increasing temperature internal diameter decreased while wall thickness increased at the expense of nanotubes length [103].

As shown in Fig. 8, the conductivity along the TiO_2 nanotubes with three different thickness is strongly affected by annealing temperature. Smallest resistance is observed at about 350–450 °C when the amorphous nanotube arrays are totally converted into anatase layers [99]. And it is evident to see that specific resistivity increases with thicker nanotube arrays which can be shown more clearly in the inset in Fig. 8. Furthermore, calcination temperature is responsible for the decrease in the length of the anatase TiO_2 nanotubes. As shown in Fig. 9a, increment of temperature between 300 and 500 °C causes the as-prepared nanotube arrays slightly changing in thickness from 13.6 to 12.6 μm. When annealing temperature continuously increases to 600 °C, the average length of the nanotubes decrease dramatically to 6.6 μm. Figure 9b shows conversion from anatase TiO_2 to rutile phase TiO_2 occuring at 500 °C when the rutile barrier layer is formed on the bottom of the TiO_2 nanotube arrays along the anatase nanotubes by consuming the bottom layer if the annealed temperature is further increased. This leads to a length decrease and corresponding photocatalytic activity decline [104].

Doping

Doping ions or atoms into titania lattice, a substitution within the lattice either at Ti^{4+} or O^{2-} sites, on the one hand, changes the lattice constants and bond energy. On the other hand, it is beneficial to the separation between photogenerated electron and hole pair, which in turn adjusts the band gap and improves the photoelectrochemical performance of nanotubes [15]. The impurity doping has been commonly applied to extend the light absorption onset of TiO_2 nanotubes by either introducing subbandgap states or adjusting its bandgap width [105]. Lately, co-doping approach has been proposed as a more efficient way to reduce the band gap and adjust energy band level in favor of photoelectriochemical reactions [106, 107]. There are various kinds of doped-elements and preparation methods, and Table 2 summarizes some methods and the doping effects of doped titania nanotubes.

The most typical doped TiO_2 nanotubes are as follows:

i. Metal-doped TiO_2 nanotubes such as Nb [107], Fe [108], Cu [109], Cr [110], Zr [111], Zn [112], and V [113]
ii. Non-metal-doped TiO_2 nanotubes such as N [105], F [114], B [115], C [116], S [117], and I [118]
iii. Co-doped TiO_2 nanotubes such as N–Ta [105], N–Nb [107], and C–N–Ni [119]

Choiet systematically studied the photoreactivities of 21 metal ion-doped quantum-sized TiO_2 doping with Fe, Mo, Ru, Os, Re, V, and Rh significantly increases quantum efficiency, while Co and Al doping decreases the photoreactivity [120]. Momeni et al. recently obtained Fe-TiO_2 nanotube (Fe-TNT) composites using different amounts of

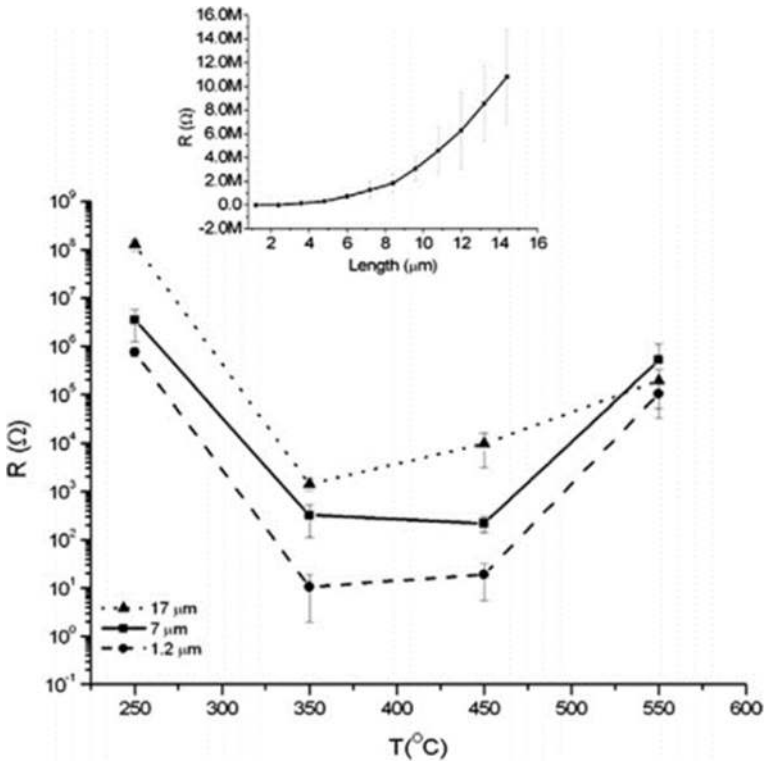

Fig. 8 Electrical resistance as a function of the annealing temperature for the different nanotube layer thicknesses. The curve shows electrical resistance measurement for different titania nanotube arrays grown in ethylene glycol based electrolyte containing HF and water at different temperature and the influence of thickness on resistance. The inset shows more details about the relationship between the thickness of the nanotube arrays annealed at 250 °C and their specific resistivity. Reproduced from ref. [99]

irons to decorate anodically formed TiO_2 nanotubes with potassium ferricyanide as the iron source, indicating that Fe doping efficiently accelerates the photocatalytic performance for water splitting [108]. Not limited to transition metals, other elements including N [105], F [114], B [115], C [116], S [117], and I [118] are successfully explored. Nitrogen-doped TiO_2 nanotubes turns out to be a promising path to narrow the band gap energy with enhanced photocurrent response in the visible light and the tube length influences the magnitude of conversion efficiency [121, 122]. Kim and co-workers proved that TaOxNy layer-decorated N-TNT (N-doped TiO_2 nanotubes) as dual modified TNTs have significantly improved both visible (3.6 times) and UV (1.8 times) activities for water splitting [105]. At present, more researches are aimed at co-doping which exhibits remarkable synergistic effect causing a significant improvement on photoelectriochemical properties. Chai et al. grew Gd–La co-doped TiO_2 nanotubes by an ultrasonic hydrothermal method, enhancing visible light photocatalysts [123]. Cottineau et al. modified titania nanotubes with nitrogen and niobium to achieve co-doped nanotubes with noticeably enhanced photoelectriochemical conversion efficiency in the visible light range [107]. Nevertheless, the mechanism for increasing photoconductivity and synergistic effect of various elements on co-doping remains a further study.

Surface Modification

Surface modification means decoration on surface of TiO_2 nanotube arrays with nanoparticles (metal, semiconductors, and organic dyes). Nanowire arrays can also be fabricated by electrodeposition into titanium oxide nanotubes [124]. TiO_2 nanotube is a semiconductor with a wide band gap, which can only absorb ultraviolet light [97, 125]. Any other nanomaterials which possess a narrow band gap or can absorb the visible light can be used as a sensitizer for titania nanotubes. Silver nanoparticles can be decorated on the tube wall by soaking the titania nanotube arrays in $AgNO_3$ solutions and photocatalytically reducing Ag^+ on a TiO_2 surface by UV illumination [126]. Ag/TiO_2 nanotubes show a significantly higher photocatalytic activity and good biological performance compared with neat TiO_2 nanotubes [126, 127]. Some compositions such as graphene oxide GO [128], CdS [129], CdSe [130], and $ZnFe_2O_4$ [131]. can be modified on TiO_2 nanotube arrays. Lately, GO have

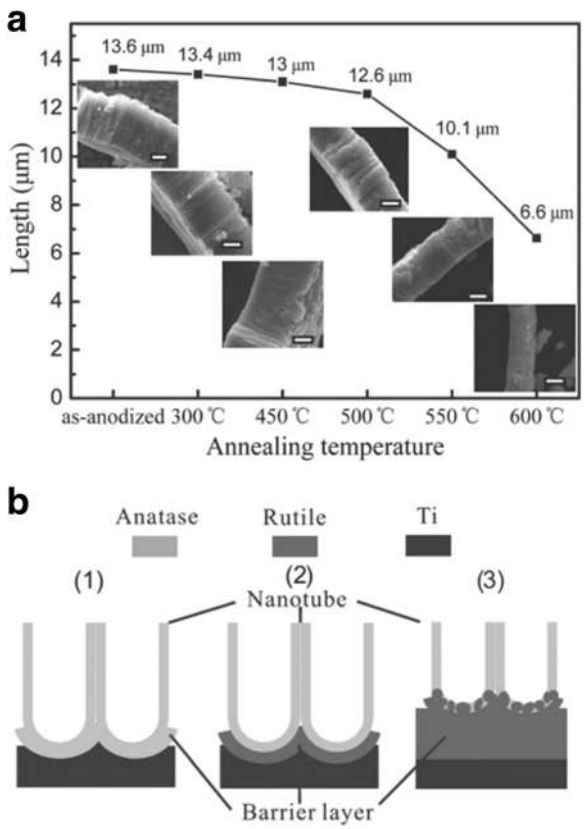

Fig. 9 Evolution of titania nanotube arrays at different calcination temperatures. The electrolyte was ethylene glycol containing 0.3 wt% ammonium fluoride and 5 vol% distilled water. **a** The decrease in the thickness of titania nanotube arrays at different annealing temperature from 300 to 600 °C. The insets are corresponding SEM images and the scale bar is 5 μm. **b** The schematic of crystallization process of anodic titania nanotubes annealed at (1) 450 °C, (2) 500 °C, and (3) 600 °C in air. Reproduced from ref. [104]

attracted much scientific interest in nanoscale devices and sensors which is easy to combine with nanostructure materials to compose some compounds. Titania nanotubes fabricated by anodization in water-ethylene glycol electrolyte consisting of 0.5 wt% ammonium fluoride (NH_4F) can be incorporated with GO by cyclic voltammetric method, which achieve higher photocatalytic activity and more effective conversion efficiency (GO-modified vs pure nanotubes = 26.55%:7.3%) of solar cell than unmodified TiO_2 nanotubes [128]. Semiconductor composite is a method improving the performance of titania nanotubes via, in some specific way, combining two kinds of semiconductors with different band gap [132]. Yang et al. decorated CdSe nanoparticles on the surface of TiO_2 nanotubes by applying an external electric field to accelerate CdSe nanoparticles in nanochannels resulting in a material with more stable and higher photoresponse to visible light. Furthermore, the degeneration rate of anthracene-9-carbonxylic acid when exposed to the green light irradiation indicating that CdSe dominates the photocatalytic process under visible light [130].

Besides, other oxide nanoparticle deposition such as WO_3 [133] or TiO_2 [134] onto TiO_2 nanotubes by the hydrolysis of a chloride precursor also turns out to augment the surface area and improve the solar cell efficiency. Another very effective approach is to consider organic dyes as sensitizers for TiO_2 nanotubes to improve its optical properties [135]. Lately, atomic layer deposition (ALD) becomes an established procedure to modify TiO_2 nanotube layers. ALD appears to be a very uniform and precisely controllable deposition process to functionalize nanotubes in conformably coating the surface of the nanotube layers with one atomic layer after another of a secondary material, such as Pd [136], ZnO [137], Al_2O_3 [138], CdS [139], or TiO_2 [140].

Biomedical Applications

Historically, the mentioned milestones were reported on the fabrication of titania nanotube arrays contributing to widen the promising applications over the past 20 years in the areas ranging from anticorrosion, self-cleaning coatings, and paints to sensors [141–143], dye-sensitized and solid-state bulk heterojunction solar cells [144–146], photocatalysis [147, 148], eletrocatalysis, and water photoelectrolysis [149, 150]. They also outperform in biomedical directions as biocompatible materials, toward biomedical coatings with enhanced osseointegration, drug delivery systems, and advanced tissue engineering [15, 135, 141, 142, 151]. In the following section, we will give an overview of current efforts toward TiO_2 nanotubes biomedical applications. Titania nanotubes possess good biocompatibility as they show some antibacterial property, low cytotoxicity, good stability, and cytocompatibility including promoting adhesion, proliferation, and differentiation of osteoblast and mesenchymal stem cells (MSCs) with a high surface area-to-volume ratio and controllable dimensions [152–155].

However, Ti products have inadequate antibacterial ability and efforts have been made to improve their antibacterial properties such as modifications on titania nanotubes for biomedical applications like bioimplant [126, 156].

Biological Coatings And Interactions with Cells

A number of in vitro and in vivo studies have demonstrated that MSCs, osteoblasts and osteoclasts show size-selective response which means the effect of size holds an important position in cell interaction where the optimized size for cell adhesion, proliferation,

Table 2 Some doped-elements, preparation methods, and the doping effects of doped titania nanotubes as based on the classification of metal-doping, non-metal doping, and co-doping

Classification	Raw material	Synthesis	Element	Doping effect	Ref
Metal doping	$K_3Fe(CN)_6$	One-step anodizing 60 V 6 h at 25 °C	Fe	Band gap: 2.85/2.65/2.10/2.03 eV (undoped: 3.18 eV) photocurrent density: 930/1320/675/590 μA cm^{-2} (undoped: < 240 μA cm^{-2}) at 1.5 V under visible light more stable and high photoresponse to visible light	[108]
	$Cu(NO_3)_2{\cdot}3H_2O$	One-step anodizing 20 V 1 h at room temperature	Cu	Band gap: 2.65 eV (undoped: 3.20 eV) total amount of H_2 evolved: 29 μL cm^{-2} 2 h (undoped: 7.6 μL cm^{-2} 2 h) higher decomposition rate of methylene blue higher stability after multiple reuses	[109]
	K_2CrO_4	One-step anodizing 60 V 6 h at 25 °C	Cr	Band gap: 2.82/2.71/2.30 eV (undoped: 3.20 eV) photocurrent density: 360/280/190 μA cm^{-2} (undoped: < 39 μA cm^{-2}) at 1.0 V under visible light total amount of H_2 evolved: 37/28/12 μL cm^{-2} 4 h (undoped: ≈ 0 μL cm^{-2}) higher stability after multiple reuses	[110]
	$Zr(NO_3)_4$	Two-step anodizing 3/7/10/15 V 1 h	Zr	Higher photocatalytic activities than that of pure TiO_2 nanotube arrays good photocatalytic stability and could be reused	[111]
	ZnF_2	One-step anodizing 30 V 15 h at 25 °C	Zn	Band gap: 2.86/2.84 eV (undoped: 3.00 eV) degeneration rate of methylene blue under visible light for 10 h:88/66% (undoped: ≈ 62%)	[112]
	V_2O_5	One-pot hydrothermal method at 130 °C 3 h	V	Band gap: 2.91 eV (undoped: 3.18 eV) increased photocurrent density reaction rate (K_{app})of rhodamine B: 3 ~ 9 fold as compared to undoped one under UV and visible light	[113]
Non-metal doping	NH_3	Annealing a flow rate of 400 mL min^{-1} at 500 °C 3 h	N	Band gap: 2.8 eV (undoped: 3.1 eV) Table2: Some doped-elements, preparation methods, and the doping effects of doped titania nanotubes as a based on the classification of metal-doping, non-metal doping, and co-doping. Table 2: Some doped-elements, preparation methods, and the doping effects of doped titania nanotubes as a based on the classification of metal-doping, non-metal doping, and co-doping. Photocurrent density: 1.4 mA cm^{-2} (undoped: 1.6 mA cm^{-2}) at 0.9 V under UV-enhanced PEC activities under visible light and decreased UV light absorption	[105]
	H_2TiF_6	Spray pyrolysis	F	Enhancement of surface acidity and creation of oxygen vacancies, increase of active sites	[114]
	H_3BO_3	Anodizing 1.8 V 15-60 min	B	Band gap: 2.91 eV (undoped: 3.20 eV), photocurrent density: 311 μA cm^{-2} (undoped: 41.7 μA cm^{-2}) at − 0.6 ~ 0.9 V under UV	[115]
	CH_4	Calcination at 820 °C 18 min in natural gas flame	C	Band gap: 2.84 eV (undoped: 2.92 eV) an additional intragap band: 1.30 eV increased lifetime of photogenerated carriers in the UV	[116]
	$K_2S_2O_5$	One-step anodizing 20 V 1 h at 25 °C	S	Band gap: 2.61 eV (undoped: 3.20 eV) high stability after multiple reuses photocurrent density: > 1.22 mA cm^{-2} (undoped:< 0.19 mA cm^{-2}) at 1.50 V under visible light total amount of H_2 evolved: 41 μL cm^{-2} 4 h (undoped: ≈ 0 μL cm^{-2})	[117]
	KI、HIO_4	Two-step anodizing 1.5 V 15 min at 23 ± 1 °C	I	Band gap: 2.95/3.0 eV (undoped: 3.07 eV) enhanced photocurrent density under both visible and UV illumination degeneration rate of methylene blue under visible light for 2 h: 71/65% (undoped: ≈ 31%)	[118]
Co-doping	NH_3 $TaCl_5$	Drop-casting method at 450 °C 30 min	N-Ta	Band gap: 2.5 eV (undoped: 3.1 eV) photocurrent density: 2.5 mA cm^{-2} (undoped: 1.6 mA cm^{-2}) at 0.9 V under UV-enhanced PEC activities under both visible and UV illumination	[105]
	NH_3 $(NH_4)_5[(NbOF_4)(NbF_7)_2]$	Anodizing 45 V at 25 ± 1 °C annealing a flow	N-Nb	Strongly enhanced PEC activities for water splitting under both visible light and UV light	[107]

Table 2 Some doped-elements, preparation methods, and the doping effects of doped titania nanotubes as based on the classification of metal-doping, non-metal doping, and co-doping *(Continued)*

Classification	Raw material	Synthesis	Element	Doping effect	Ref
		rate of 100cm^3 min^{-1} at 550 °C 2 h			
	$K_2[Ni(CN)_4]$	Anodizing 40 V 2 h at room temperature	Ni-N-C	Band gap: 2.588 ~ 2.972 eV (undoped: 3.062 eV) photocurrent density: 10 times greater than that of undoped one under visible light	[119]

growth, and differentiation is ranging from 15 to 100 nm [153, 157, 158]. Particularly, it was demonstrated that the TiO_2 nanotubes with a diameter of 70 nm was the optimal nanoscale geometry for the osteogenic differentiation of human adipose-derived stem cells (hASCs) [159]. Smith et al. reported increased dermal fibroblasts and decreased epidermal keratinocyte adhesion, proliferation, and differentiation on TiO_2 nanotube arrays (diameter 70–90 nm, length 1–1.5 μm) [160]. As shown in Fig. 10, Peng et al. found that nanotubular surface preferentially promoted proliferation and function in endothelial cells (EC) while decreased in vascular smooth muscle cell (VSMC) by measuring EdU, a thymidine analog which is incorporated by proliferating cells [161]. Furthermore, it is pointed out that surface wettability of the TiO_2 nanotube layers is recognized as a critical factor for cell behavior which can be adjusted by changing the diameter of the nanotubes. That is to say, water contact angles can be altered without changing the surface chemistry [158]. To get further understanding of the effect of TiO_2 nanotube layers to bone-forming cells as well as stem cells response, Park et al. seeded green fluorescent protein-labeled rat MSCs on TiO_2 nanotube layers with six different diameters (15, 20, 30, 50, 70, and 100 nm), resulting in cell activity that is sensitive to nanoscale surface topography with a maximum in cell activity obtained for tube diameters of approximately 15–30 nm. Such lateral spacing exactly corresponds to the predicted lateral spacing of integrin receptors in focal contacts on the extracellular matrix, forcing clustering of integrins into the closest packing, resulting in optimal integrin activation. While tube diameters larger than 50 nm, severely impaired cell spreading, adhesion, and spacing of 100 nm may lead to the cell apoptosis [94]. Besides adjusting the size of the nanotubes, surface modification loaded with bioactive factors should be highlighted, in which case biomedical properties can be further optimized. In the case of bone implants, hydroxyapatite (HA) formation is important for osseointegration. Recent works have shown hydroxyapatite nanocrystalline coating onto the nanotubular TiO_2 results in further enhanced osseointegration with strong adhesion and bond strength, and a drastic enhancement of deposition rate is observed [162, 163]. Nanotubular TiO_2 surface can greatly enhance the natural apatite growth rate in simulated body fluid (SBF) compared with flat surfaces [10, 164]. The alkaline-treated TiO_2 nanotubes with NaOH solutions are more bioactive in SBF, where sodium titanate can significantly accelerate nucleation and the growth of HA formation presenting a well-adhered bioactive surface layer on Ti due to its larger surface area and promoted mechanical interlocking between HA and TiO_2 nanotubes [165, 166]. Electrodeposited with hydroxyapatite, higher adhesion of TiO_2 nanotubes has been described in the

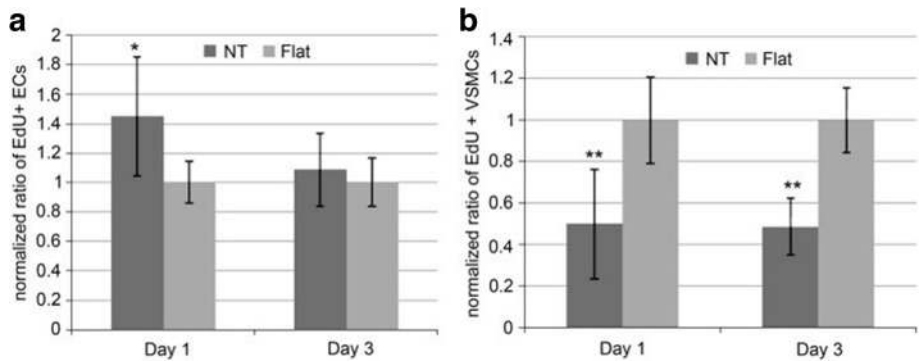

Fig. 10 Ratio of EdU positive **a** ECs and **b** VSMCs on flat or nanotube substrate. It is normalized by the average proportion of positive cells on flat surfaces on day 1 and 3. Data is presented as average ± standard deviation. *$p < 0.05$, **$p < 0.01$ versus same day flat control, $n = 6$ reproduced from ref. [161]

literature by means of adhesive tape test and the live/dead cell staining study which is essential for early bone formation [166]. The results also showed that at the length of 560 nm the highest adhesion of HA surface on the nanotubes is observed. Also the nanotube surface can indeed strengthen Collagen type I expression in vivo experiment which is considered to be a basic initial bone matrix protein in bone formation [167]. Moreover, annealing of the amorphous nanotubes to anatase or a mixture of anatase and rutile was found to be an important factor in the apatite formation process [164].

Drug Delivery and Antibacterial Ability

Furthermore, the tubular nature of TiO_2 in biomedical devices may be exploited as gene and drug delivery carriers with living matter due to its high surface area, controllable pore, and self-ordered structure [1, 15]. When the orthopedic bioimplant is placed into the bone defect, persistent and chronic infection is one of the most common and serious complications associated with biomedical implantation [16, 168]. Certain dimension and crystallinity may be useful to prevent bacteria adhesion and promote bone formation. The thermal annealing has decreased the number of bacteria adhering to the Ti surface. It could be in part because heat treatment removes the fluorine content which has a tendency to attract bacteria. The research also indicates that nanotubes with 60 or 80 nm in diameter decrease the number of live bacteria as compared to lower diameter (20 or 40 nm) nanotubes [169, 170].

Bauer et al. loaded epidermal growth factor (EGF) and bone morphogenetic protein-2(BMP-2) onto the TiO_2 nanotubes surface by covalent attachment. They observed positive influence on the behavior of MSCs on 100-nm nanotube arrays where cell count was at much higher levels compared to the untreated one [171]. Lately, titania nanotubes loaded with antibiotics contribute to suppressing bacterial infections. As gentamicin sulphate (GS) is mostly widely used with highly water solubility, Feng et al. loaded titania nanotubes with GS through physical adsorption and cyclic loading which can treat many types of bacterial infections [172]. Zhang et al. fabricated titania nanotubes loaded with vancomycin to investigate the increasing biocompatibility and obvious antibacterial effect on *Staphylococcus aureus* [173]. However, systemic antibiotics in clinical will bring many side effects. The release of antibiotics from the nanotubes is too fast to maintain the long-term antibacterial ability, and the use of antibiotics may develop resistant strains [126, 168, 174]. Ensuring a constant release rate becomes a crucial but difficult part in the field of drug delivery. In strategies like surface modification, controlling the dimension of nanotube arrays, biodegradable polymer coating have been employed to solve the issue [21]. Drug release of several drugs such as antibiotics or growth factors from titania nanotube arrays can be adjusted by varying their diameters and lengths [152, 175, 176]. Feng et al. covered a thin film comprising a mixture of GS and chitosan on GS-loaded titania nanotubes and showed a controlled release of the drug providing sustained release effects to a certain extent [172]. Titania nanotube arrays as drug nanoreservoirs on Ti surface for loading of BMP-2 were fabricated by Hu et al. and then further covered with gelatin/chitosan multilayers to control the release of the functional molecule meanwhile maintain the bioactivity for over 120 h via a spin-assisted layer-by-layer assembly technique which is mainly based on electrostatic interactions between polyanions and polycations as well as promote osteoblastic differentiation of MSCs [177]. Lai et al. successfully fabricated Chi/Gel multilayer on melatonin-loaded TiO_2 nanotube arrays to control the sustained release of melatonin and promote the osteogenic differentiation of mesenchymal stem cells [178]. Karan et al. synthesized titania nanotubes loaded with the water-insoluble anti-inflammatory drug indomethacin and modified lactic-co-glycolic acid on surface as a polymer film in order to extend the drug release time of titania nanotubes and produce favorable bone cell adhesion properties, with reduced burst release (from 77 to > 20%) and extended overall release from 4 days to more than 30 days [152]. As previous study reported that surface treatment of implants with *N*-acetyl cysteine (NAC) may reduce implant-induced inflammation and promote faster bone regeneration [179], Lee et al. examined the feasibility of *N*-acetyl cysteine-loaded titania nanotubes as a potential drug delivery system onto an implant surface, and the data indicates the enhanced osseointegration and the value of the small animal model in assessing diverse biological responses to dental implants. Besides, TiO_2 nanotube arrays are suitable for loading inorganic agents like Ag, Sr, and Zn to obtain long-term antibacterial ability and osseointegration [126, 180–182]. Ag nanoparticles have been incorporated into TiO_2 nanotube arrays previously with satisfactory small possibility to develop resistant strains, a broad-spectrum antibacterial property, low cytotoxicity, and good stability by immersion in a silver nitrate solution followed by ultraviolet light radiation [126]. Zhang et al. demonstrated that a series of porous TiO_2 coatings with different concentrations of silver had significant inhibition effect on *Escherichia coli* and *Staphylococcus aureus*. Besides, only with the

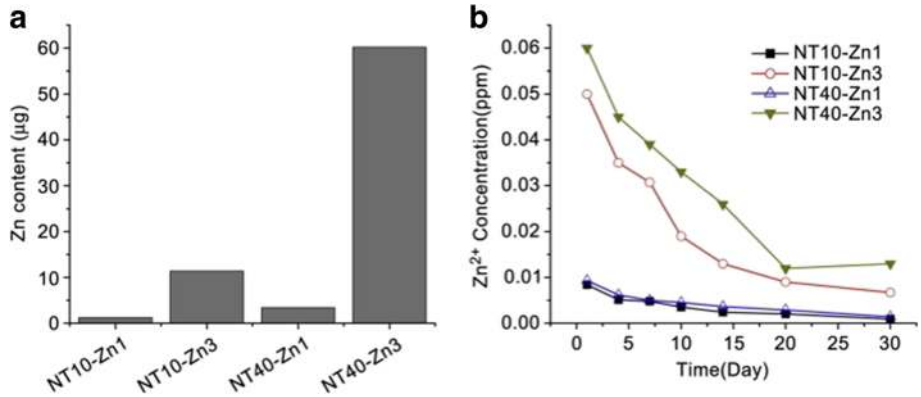

Fig. 11 **a** Total amounts of Zn incorporated into the NT-Zn samples for the 1 cm^2 coatings and **b** non-cumulative Zn release profiles from NT-Zn into PBS. Reproduced from ref. [181]

optimum amount of silver can the coatings retain the antibacterial effect but without any measurable cytotoxicity to cells [183]. Due to cytotoxicity observed by the excessive release of Ag^+ subsequently, titania nanotube arrays with Ag_2O nanoparticles embedded in the wall are prepared on Ti by TiAg magnetron sputtering and anodization in order to get slower and more controllable silver ion release [184]. That is because the TiO_2 barrier is surrounded thereby minimizing the cytotoxicity induced by burst or large Ag^+ release.

Similar to Ag, Zn possesses antibacterial and anti-inflammation properties, and osteogenesis induction [185–187]. Huo et al. produced anodic TiO_2 nanotube arrays at 10 V and 40 V (NT10 and NT40) incorporated with Zn by hydrothermal treatment at 200 °C for 1 and 3 h (NT10-Zn1, NT10-Zn3, NT40-Zn1, and NT40-Zn3) in Zn containing solutions, followed by annealing at 450 °C for 3 h in air. NT40-Zn3 has the largest Zn loading capacity and releases more Zn compared with other samples. The amounts of Zn released diminish gradually with time and nearly no Zn can be detected 1 month later except sample NT40-Zn3 (Fig. 11). The NT-Zn samples present different antibacterial ability. It is evident that NT40-Zn3 and NT10-Zn3 effectively kill more adherent bacteria as well as surrounding planktonic bacteria in the early stage. Figure 12a describes a synergistic effect of both released and surface incorporated Zn while Fig. 12b explains the effect of the released Zn [181].

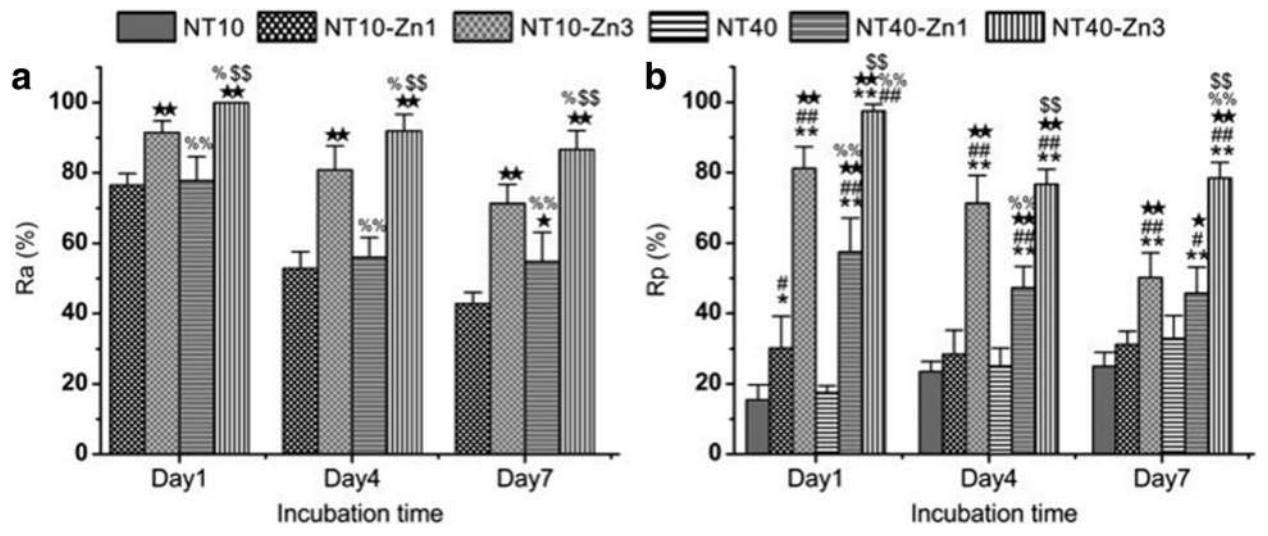

Fig. 12 **a** Antibacterial rates versus adherent bacteria on the specimen (Ra) and **b** antibacterial rates against planktonic bacteria in the medium (Rp) *, **$p < 0.05$ and 0.01 vs NT10; #, ##$p < 0.05$ and 0.01 vs NT40; ★, ★★$p < 0.05$ and 0.01 vs NT10-Zn1; %, %%$p < 0.05$ and 0.01 vs NT10-Zn3; $, $$$p < 0.05$ and 0.01 vs NT40-Zn1. Reproduced from ref. [181]

Conclusions

This review presents the historical developments and traditional formation mechanism of titania nanotube arrays grown by electrochemical anodization as well as the approaches to influence and modify morphology in order to improve their performances. We also focus on current efforts toward TiO_2 nanotubes applications in biomedical directions. Those steady progresses have demonstrated that TiO_2 nanotubes are playing and will continue to play an important role in material science, but there are still some aspects needed to be further improved.

1. The synthesis of TiO_2 nanotube arrays is already comparatively mature so far in fact, but how to simplify the technology for the purpose of large-scale production in industry with extending practical operability and how to precisely control nanotube geometry efficiently by varying the anodic parameters so as to obtain optimized properties have yet to be further investigated.
2. The formation mechanisms of anodic TiO_2 nanotubes have gradually become a hotspot of research due to their unique structure and excellent performances but the exact mechanism remains controversial. Conventional FAD explains the growth process and the porous structure of TiO_2 nanotubes, but the combination of viscous flow model and growth model of two currents can give a comprehensive explanation to the growth process. Notably, the validity of oxygen evolution resulting from electronic current has much room for investigation.
3. Modification is key for improving performances of titania nanotube arrays. Thus, we need to explore more methods for modification and take full advantage of the self-organized nanostructure. Through self-assembling inorganic, organic, metallic, and magnetic nanoparticles into or onto the tubes as nanocomposites with broad spectral response to visible light, high quantum efficiency, and stabilizing properties, applications could be widened. Currently, ALD appears to be an option to coat the titania nanotube layers homogenously and precisely from the bottom to the tube mouth, resulting in many advanced functionalities of the newly prepared nanotube layers. Nevertheless, further optimization of the ALD process toward coatings and inner fillings is demanded.
4. TiO_2 nanotube researches in biomedical directions are still in their infancy and have a long distance to go in clinical use. The biological reaction between cells and titania nanotubes has to develop from cellular level to molecular level and from morphological changes to molecular alterations. It has been shown that adhesion, spreading, and growth of osteoblast and mesenchymal stem cells strongly depends on nanotube diameter, so the regularity and principle of this phenomenon as well as other factors affecting cells' behaviors need to be further explored.

Abbreviations

ALD: Atomic layer deposition; BMP-2: Bone morphogenetic protein-2; DMSO: Dimethyl sulfoxide; DSSCs: Dye-sensitized solar cells; EBSD: Electron Backscatter Diffraction; EC: Endothelial cells; EdU: A thymidine analog; EGF: Epidermal growth factor; FAD: Conventional field-assisted dissolution; FE-SEM: Field-emission scanning electron microscopy; Fe-TNTs: Fe-doped TiO2 nanotubes; FIB: Focused ion beam; GO: Graphene oxide; GS: Gentamicin sulphate; HA: Hydroxyapatite; hASCs: Adipose-derived stem cells; IPCE: Incident photon-to-electron conversion efficiency; MSCs: Mesenchymal stem cells; NAC: *N*-Acetyl cysteine; N-TNT: N-doped TiO2 nanotubes; PEC: Photoelectriochemical; SBF: Simulated body fluid; UV: Ultraviolet; VSMC: Vascular smooth muscle cell

Acknowledgements

My deepest gratitude goes first and foremost to Professor Anchun Mo, my supervisor, for his constant encouragement and guidance.
Second, I thank the Department of Implantology, West China Hospital of Stomatology, Sichuan University for all the support.

Funding

Authors declare that there is no funding for the review.

Authors' Contributions

AM conceived of the study and supervised the whole study. YF drafted the manuscript including the design of the figures. Both authors read and approved the final manuscript.

Competing Interests

The authors declare that they have no competing interests.

Publisher's Note

Received: 20 October 2017 Accepted: 7 June 2018
Published online: 28 June 2018

References

1. Roy P, Berger S, Schmuki P (2011) TiO_2 nanotubes: synthesis and applications. Angew Chem Int Ed 50(13):2904–2939
2. Paramasivam I, Jha H, Liu N et al (2012) A review of Photocatalysis using self-organized TiO_2 nanotubes and other ordered oxide nanostructures. Small 8(20):3073–3103
3. Roy P, Kim D, Lee K et al (2010) TiO_2 nanotubes and their application in dye-sensitized solar cells. Nanoscale 2(1):45–59
4. Zhang Q, Cao G (2011) Nanostructured photoelectrodes for dye-sensitized solar cells. Nano Today 6(1):91–109
5. Li Y, Yu X, Yang Q. Fabrication of Nanotube Thin Films and Their Gas Sensing Properties[J]. Journal of Sensors. 2009;2009(2009):19.
6. Ochiai T, Fujishima A (2012) Photoelectrochemical properties of TiO_2 photocatalyst and its applications for environmental purification. J Photochem Photobiol C: Photochem Rev 13(4):247–262
7. Maher S, Qin J, Gulati K, et al. 3D printed titanium implants with nano-engineered surface titania nanotubes for localized drug delivery[J]. Chemeca 2016: Chemical Engineering-Regeneration, Recovery and Reinvention. 2016;65-76.
8. Fujishima A, Honda K (1972) Electrochemical photolysis of water at a semiconductor electrode. nature 238(5358):37–38
9. Fujishima A, Rao TN, Tryk DA (2000) Titanium dioxide photocatalysis. J Photochem Photobiol C: Photochem Rev 1(1):1–21

10. Tryk DA, Fujishima A, Honda K (2000) Recent topics in photoelectrochemistry: achievements and future prospects. Electrochim Acta 45(15):2363–2376
11. Li X, Wang L, Fan Y et al (2012) Biocompatibility and toxicity of nanoparticles and nanotubes. J Nanomater 2012:6
12. Iijima S, Ichihashi T (1993) Single-shell carbon nanotubes of 1-nm diameter. nature 363(6430):603–605
13. Assefpour-Dezfuly M, Vlachos C, Andrews EH (1984) Oxide morphology and adhesive bonding on titanium surfaces. J Mater Sci 19(11):3626–3639
14. Zwilling V, Aucouturier M, Darque-Ceretti E (1999) Anodic oxidation of titanium and TA6V alloy in chromic media. An electrochemical approach. Electrochim Acta 45(6):921–929
15. Lee K, Mazare A, Schmuki P (2014) One-dimensional titanium dioxide nanomaterials: nanotubes. Chem Rev 114(19):9385–9454
16. Kasuga T, Hiramatsu M, Hoson A et al (1999) Titania nanotubes prepared by chemical processing. Adv Mater 11(15):1307–1311
17. Yang J, Mei S, Ferreira JMF (2001) Hydrothermal synthesis of TiO2 nanopowders from tetraalkylammonium hydroxide peptized sols. Mater Sci Eng C 15(1):183–185
18. Chae SY, Park MK, Lee SK et al (2003) Preparation of size-controlled TiO2 nanoparticles and derivation of optically transparent photocatalytic films. Chem Mater 15(17):3326–3331
19. Lakshmi BB, Dorhout PK, Martin CR (1997) Sol–gel template synthesis of semiconductor nanostructures. Chem Mater 9(3):857–862
20. Jung JH, Kobayashi H, van Bommel KJC et al (2002) Creation of novel helical ribbon and double-layered nanotube TiO2 structures using an organogel template. Chem Mater 14(4):1445–1447
21. Losic D, Aw MS, Santos A et al (2015) Titania nanotube arrays for local drug delivery: recent advances and perspectives. Expert opinion on drug delivery 12(1):103–127
22. Qiu X, Howe JY, Cardoso MB et al (2009) Size control of highly ordered HfO_2 nanotube arrays and a possible growth mechanism. Nanotechnology 20(45):455601
23. Jiang W, He J, Zhong J et al (2014) Preparation and photocatalytic performance of ZrO_2 nanotubes fabricated with anodization process. Appl Surf Sci 307:407–413
24. Liu X, Yuan R, Liu Y et al (2016) Niobium pentoxide nanotube powder for efficient dye-sensitized solar cells. New J Chem 40(7):6276–6280
25. Gonçalves RV, Migowski P, Wender H et al (2012) Ta_2O_5 nanotubes obtained by anodization: effect of thermal treatment on the photocatalytic activity for hydrogen production. J Phys Chem C 116(26):14022–14030
26. Yang Y, Albu SP, Kim D et al (2011) Enabling the anodic growth of highly ordered V2O5 nanoporous/nanotubular structures. Angew Chem Int Ed 50(39):9071–9075
27. Berger S, Tsuchiya H, Schmuki P (2008) Transition from nanopores to nanotubes: self-ordered anodic oxide structures on titanium–aluminides. Chem Mater 20(10):3245–3247
28. Yasuda K, Schmuki P (2007) Electrochemical formation of self-organized zirconium titanate nanotube multilayers. Electrochem Commun 9(4): 615–619
29. Wang X, Li Z, Shi J et al (2014) One-dimensional titanium dioxide nanomaterials: nanowires, nanorods, and nanobelts. Chem Rev 114(19): 9346–9384
30. Liu B, Aydil ES (2009) Growth of oriented single-crystalline rutile TiO2 nanorods on transparent conducting substrates for dye-sensitized solar cells. J Am Chem Soc 131(11):3985–3990
31. Fattakhova-Rohlfing D, Zaleska A, Bein T. Threedimensional titanium dioxide nanomaterials[J]. Chemical reviews. 2014;114(19):9487-9558.
32. Chen X, Mao SS (2007) Titanium dioxide nanomaterials: synthesis, properties, modifications, and applications. Chem Rev 107(7):2891–2959
33. Macak JM, Tsuchiya H, Ghicov A et al (2007) TiO_2 nanotubes: self-organized electrochemical formation, properties and applications. Curr Opinion Solid State Mater Sci 11(1–2):3–18
34. Yang LX, Luo SL, Cai QY et al (2010) A review on TiO_2 nanotube arrays: fabrication, properties, and sensing applications. Chin Sci Bull 55(4–5):331–338
35. Paulose M, Mor GK, Varghese OK et al (2006) Visible light photoelectrochemical and water-photoelectrolysis properties of titania nanotube arrays. J Photochem Photobiol A Chem 178(1):8–15
36. Berger S, Hahn R, Roy P et al (2010) Self-organized TiO_2 nanotubes: factors affecting their morphology and properties. Phys Status Solidi B 247(10): 2424–2435
37. Jha H, Roy P, Hahn R et al (2011) Fast formation of aligned high-aspect ratio TiO_2 nanotube bundles that lead to increased open circuit voltage when used in dye sensitized solar cells. Electrochem Commun 13(3): 302–305
38. Albu SP, Kim D, Schmuki P (2008) Growth of aligned TiO2 bamboo-type nanotubes and highly ordered nanolace. Angew Chem 120(10):1942–1945
39. Song YY, Schmuki P (2010) Modulated TiO_2 nanotube stacks and their use in interference sensors. Electrochem Commun 12(4):579–582
40. Albu SP, Ghicov A, Aldabergenova S et al (2008) Formation of double-walled TiO_2 nanotubes and robust Anatase membranes. Adv Mater 20(21): 4135–4139
41. Paulose M, Prakasam HE, Varghese OK et al (2007) TiO_2 nanotube arrays of 1000 μm length by anodization of titanium foil: phenol red diffusion. J Phys Chem C 111(41):14992–14997
42. Masuda H, Fukuda K (1995) Ordered metal nanohole arrays made by a two-step replication of honeycomb structures of anodic alumina. science 268(5216):1466
43. Macak JM, Albu SP, Schmuki P (2007) Towards ideal hexagonal self-ordering of TiO_2 nanotubes. physica status solidi (RRL)-Rapid Research Letters 1(5): 181–183
44. Sopha H, Jäger A, Knotek P et al (2016) Self-organized anodic TiO_2 nanotube layers: influence of the Ti substrate on nanotube growth and dimensions. Electrochim Acta 190:744–752
45. Leonardi S, Li Bassi A, Russo V et al (2011) TiO_2 nanotubes: interdependence of substrate grain orientation and growth characteristics. J Phys Chem C 116(1):384–392
46. Macak JM, Jarosova M, Jäger A et al (2016) Influence of the Ti microstructure on anodic self-organized TiO2 nanotube layers produced in ethylene glycol electrolytes. Appl Surf Sci 371:607–612
47. Kondo T, Nagao S, Yanagishita T et al (2015) Ideally ordered porous TiO_2 prepared by anodization of pretextured Ti by nanoimprinting process. Electrochem Commun 50:73–76
48. Kondo T, Nagao S, Hirano S et al (2016) Fabrication of ideally ordered anodic porous TiO_2 by anodization of pretextured two-layered metals. Electrochem Commun 72:100–103
49. Sopha H, Samoril T, Palesch E et al (2017) Ideally hexagonally ordered TiO_2 nanotube arrays. ChemistryOpen 6(4):480–483
50. Diggle JW, Downie TC, Goulding CW (1969) Anodic oxide films on aluminum. Chem Rev 69(3):365–405
51. Jing W, Haowen F, He Z et al (2016) Anodizing process of titanium and formation mechanism of anodic TiO_2 nanotubes. Progress in Chemistry 28(2–3):284–295
52. Fahim NF, Sekino T, Morks MF et al (2009) Electrochemical growth of vertically-oriented high aspect ratio titania nanotubes by rabid anodization in fluoride-free media. J Nanosci Nanotechnol 9(3):1803–1818
53. Houser JE, Hebert KR (2009) The role of viscous flow of oxide in the growth of self-ordered porous anodic alumina films. Nat Mater 8(5):415
54. Gong D, Grimes CA, Varghese OK et al (2001) Titanium oxide nanotube arrays prepared by anodic oxidation. J Mater Res 16(12):3331–3334
55. Mor GK, Varghese OK, Paulose M et al (2003) Fabrication of tapered, conical-shaped titania nanotubes. J Mater Res 18(11):2588–2593
56. Varghese OK, Gong D, Paulose M et al (2003) Extreme changes in the electrical resistance of titania nanotubes with hydrogen exposure. Adv Mater 15(7–8):624–627
57. Cai Q, Paulose M, Varghese OK et al (2005) The effect of electrolyte composition on the fabrication of self-organized titanium oxide nanotube arrays by anodic oxidation. J Mater Res 20(1):230–236
58. Macak JM, Sirotna K, Schmuki P (2005) Self-organized porous titanium oxide prepared in Na_2SO_4/NaF electrolytes. Electrochim Acta 50(18):3679–3684
59. Macak JM, Tsuchiya H, Taveira L et al (2005) Smooth anodic TiO_2 nanotubes. Angew Chem Int Ed 44(45):7463–7465
60. Paulose M, Shankar K, Yoriya S et al (2006) Anodic growth of highly ordered TiO_2 nanotube arrays to 134 μm in length. J Phys Chem B 110(33):16179–16184
61. Shankar K, Mor GK, Fitzgerald A et al (2007) Cation effect on the electrochemical formation of very high aspect ratio TiO2 nanotube arrays in formamide–water mixtures. J Phys Chem C 111(1):21–26
62. Yoriya S, Mor GK, Sharma S et al (2008) Synthesis of ordered arrays of discrete, partially crystalline titania nanotubes by Ti anodization using diethylene glycol electrolytes. J Mater Chem 18(28):3332–3336
63. Wan J, Yan X, Ding J et al (2009) Self-organized highly ordered TiO2 nanotubes in organic aqueous system. Mater Charact 60(12):1534–1540

64. Sulka GD, Kapusta-Kołodziej J, Brzózka A et al (2013) Anodic growth of TiO_2 nanopore arrays at various temperatures. Electrochim Acta 104:526–535
65. Albu SP, Ghicov A, Macak JM et al (2007) 250 μm long anodic TiO_2 nanotubes with hexagonal self-ordering. physica status solidi (RRL)-Rapid Research Letters 1(2)
66. Raja KS, Gandhi T, Misra M (2007) Effect of water content of ethylene glycol as electrolyte for synthesis of ordered titania nanotubes. Electrochem Commun 9(5):1069–1076
67. Macak JM, Hildebrand H, Marten-Jahns U et al (2008) Mechanistic aspects and growth of large diameter self-organized TiO_2 nanotubes. J Electroanal Chem 621(2):254–266
68. Enachi M, Tiginyanu I, Sprincean V et al (2010) Self-organized nucleation layer for the formation of ordered arrays of double-walled TiO_2 nanotubes with temperature controlled inner diameter. physica status solidi (RRL)-Rapid Research Letters 4(5–6):100–102
69. John SE, Mohapatra SK, Misra M (2009) Double-wall anodic titania nanotube arrays for water photooxidation. Langmuir 25(14):8240–8247
70. Ji Y, Lin K C, Zheng H, et al. Fabrication of double-walled TiO2 nanotubes with bamboo morphology via one-step alternating voltage anodization[J]. Electrochemistry Communications. 2011;13(9):1013-1015.
71. So S, Hwang I, Schmuki P (2015) Hierarchical DSSC structures based on "single walled" TiO_2 nanotube arrays reach a back-side illumination solar light conversion efficiency of 8%. Energy Environ Sci 8(3):849–854
72. Mirabolghasemi H, Liu N, Lee K et al (2013) Formation of 'single walled'TiO_2 nanotubes with significantly enhanced electronic properties for higher efficiency dye-sensitized solar cells. Chem Commun 49(20):2067–2069
73. Allam NK, Grimes CA (2007) Formation of vertically oriented TiO_2 nanotube arrays using a fluoride free HCl aqueous electrolyte. J Phys Chem C 111(35): 13028–13032
74. Allam NK, Shankar K, Grimes CA (2008) Photoelectrochemical and water photoelectrolysis properties of ordered TiO_2 nanotubes fabricated by Ti anodization in fluoride-free HCl electrolytes. J Mater Chem 18(20):2341–2348
75. Paramasivam I, Macak JM, Selvam T et al (2008) Electrochemical synthesis of self-organized TiO2 nanotubular structures using an ionic liquid (BMIM-BF4). Electrochim Acta 54(2):643–648
76. Galiński M, Lewandowski A, Stępniak I (2006) Ionic liquids as electrolytes. Electrochim Acta 51(26):5567–5580
77. Zhang G, Huang H, Zhang Y et al (2007) Highly ordered nanoporous TiO_2 and its photocatalytic properties. Electrochem Commun 9(12):2854–2858
78. Prakasam HE, Shankar K, Paulose M et al (2007) A new benchmark for TiO_2 nanotube array growth by anodization. J Phys Chem C 111(20):7235–7241
79. Sopha H, Hromadko L, Nechvilova K et al (2015) Effect of electrolyte age and potential changes on the morphology of TiO_2 nanotubes. J Electroanal Chem 759:122–128
80. Bauer S, Kleber S, Schmuki P (2006) TiO2 nanotubes: tailoring the geometry in H3PO4/HF electrolytes. Electrochem Commun 8(8):1321–1325
81. Lockman Z, Sreekantan S, Ismail S et al (2010) Influence of anodisation voltage on the dimension of titania nanotubes. J Alloys Compd 503(2):359–364
82. Wang J, Lin Z (2009) Anodic formation of ordered TiO_2 nanotube arrays: effects of electrolyte temperature and anodization potential. J Phys Chem C 113(10):4026–4030
83. LeClere DJ, Velota A, Skeldon P et al (2008) Tracer investigation of pore formation in anodic titania. J Electrochem Soc 155(9):C487–C494
84. Valota A, LeClere DJ, Hashimoto T et al (2008) The efficiency of nanotube formation on titanium anodized under voltage and current control in fluoride/glycerol electrolyte. Nanotechnology 19(35):355701
85. Ghicov A, Schmuki P (2009) Self-ordering electrochemistry: a review on growth and functionality of TiO_2 nanotubes and other self-aligned MO_x structures. Chem Commun 20:2791–2808
86. Crawford GA, Chawla N, Das K et al (2007) Microstructure and deformation behavior of biocompatible TiO_2 nanotubes on titanium substrate. Acta Biomater 3(3):359–367
87. Ghicov A, Tsuchiya H, Macak JM et al (2005) Titanium oxide nanotubes prepared in phosphate electrolytes. Electrochem Commun 7(5):505–509
88. Masuda H, Satoh M (1996) Fabrication of gold nanodot array using anodic porous alumina as an evaporation mask. Jpn J Appl Phys 35(1B):L126
89. Li D, Chang PC, Chien CJ et al (2010) Applications of tunable TiO_2 nanotubes as nanotemplate and photovoltaic device. Chem Mater 22(20): 5707–5711
90. Chen Q, Xu D, Wu Z et al (2008) Free-standing TiO_2 nanotube arrays made by anodic oxidation and ultrasonic splitting. Nanotechnology 19(36):365708
91. Li S, Zhang G, Guo D et al (2009) Anodization fabrication of highly ordered TiO_2 nanotubes. J Phys Chem C 113(29):12759–12765
92. Das S, Zazpe R, Prikryl J et al (2016) Influence of annealing temperatures on the properties of low aspect-ratio TiO_2 nanotube layers. Electrochim Acta 213:452–459
93. Krbal M, Kucharik J, Sopha H et al (2016) Charge transport in anodic TiO2 nanotubes studied by terahertz spectroscopy. physica status solidi (RRL)-Rapid Research Letters 10(9):691–695
94. Park J, Bauer S, von der Mark K et al (2007) Nanosize and vitality: TiO_2 nanotube diameter directs cell fate. Nano Lett 7(6):1686–1691
95. Prida VM, Manova E, Vega V et al (2007) Temperature influence on the anodic growth of self-aligned titanium dioxide nanotube arrays. J Magn Magn Mater 316(2):110–113
96. Macak JM, Schmuki P (2006) Anodic growth of self-organized anodic TiO2 nanotubes in viscous electrolytes. Electrochim Acta 52(3):1258–1264
97. Linsebigler AL, Lu G, Yates JT Jr (1995) Photocatalysis on TiO_2 surfaces: principles, mechanisms, and selected results. Chem Rev 95(3):735–758
98. Fan X, Wan J, Liu E et al (2015) High-efficiency photoelectrocatalytic hydrogen generation enabled by Ag deposited and Ce doped TiO_2 nanotube arrays. Ceram Int 41(3:5107–5116
99. Tighineanu A, Ruff T, Albu S et al (2010) Conductivity of TiO_2 nanotubes: influence of annealing time and temperature. Chem Phys Lett 494(4):260–263
100. Tighineanu A, Albu SP, Schmuki P (2014) Conductivity of anodic TiO2 nanotubes: influence of annealing conditions. physica status solidi (RRL)-Rapid Research Letters 8(2):158–162
101. Jaroenworaluck A, Regonini D, Bowen CR et al (2010) A microscopy study of the effect of heat treatment on the structure and properties of anodised TiO2 nanotubes. Appl Surf Sci 256(9):2672–2679
102. Varghese OK, Gong D, Paulose M et al (2003) Crystallization and high-temperature structural stability of titanium oxide nanotube arrays. J Mater Res 18(1):156–165
103. Xiao P, Liu D, Garcia BB et al (2008) Electrochemical and photoelectrical properties of titania nanotube arrays annealed in different gases. Sensors Actuators B Chem 134(2):367–372
104. Zhang X, Huo K, Wang H et al (2011) Influence of structure parameters and crystalline phase on the photocatalytic activity of TiO_2 nanotube arrays. J Nanosci Nanotechnol 11(12):11200–11205
105. Kim H, Monllor-Satoca D, Kim W et al (2015) N-doped TiO_2 nanotubes coated with a thin TaOxNy layer for photoelectrochemical water splitting: dual bulk and surface modification of photoanodes. Energy Environ Sci 8(1):247–257
106. Long R, English NJ (2009) Band gap engineering of (N, Ta)-codoped TiO_2: a first-principles calculation. Chem Phys Lett 478(4):175–179
107. Cottineau T, Béalu N, Gross PA et al (2013) One step synthesis of niobium doped titania nanotube arrays to form (N, Nb) co-doped TiO_2 with high visible light photoelectrochemical activity. J Mater Chem A 1(6):2151–2160
108. Momeni MM, Ghayeb Y (2015) Fabrication, characterization and photoelectrochemical behavior of Fe–TiO_2 nanotubes composite photoanodes for solar water splitting. J Electroanal Chem 751:43–48
109. Momeni MM, Ghayeb Y, Ghonchegi Z (2015) Fabrication and characterization of copper doped TiO_2 nanotube arrays by in situ electrochemical method as efficient visible-light photocatalyst. Ceram Int 41(7):8735–8741
110. Momeni MM, Ghayeb Y (2015) Photoelectrochemical water splitting on chromium-doped titanium dioxide nanotube photoanodes prepared by single-step anodizing. J Alloys Compd 637:393–400
111. Liu H, Liu G, Zhou Q (2009) Preparation and characterization of Zr doped TiO_2 nanotube arrays on the titanium sheet and their enhanced photocatalytic activity. J Solid State Chem 182(12):3238–3242
112. Benjwal P, Kar KK (2015) One-step synthesis of Zn doped titania nanotubes and investigation of their visible photocatalytic activity. Mater Chem Phys 160:279–288
113. Lu D, Zhao B, Fang P et al (2015) Facile one-pot fabrication and high photocatalytic performance of vanadium doped TiO_2-based nanosheets for visible-light-driven degradation of RhB or Cr (VI). Appl Surf Sci 359:435–448
114. Li D, Haneda H, Hishita S et al (2005) Fluorine-doped TiO_2 powders prepared by spray pyrolysis and their improved photocatalytic activity for decomposition of gas-phase acetaldehyde. J Fluor Chem 126(1):69–77
115. Szkoda M, Lisowska-Oleksiak A, Siuzdak K (2016) Optimization of boron-doping process of titania nanotubes via electrochemical method toward enhanced photoactivity. J Solid State Electrochem 20(6):1765–1774

116. Xu C, Shaban YA, Ingler WB et al (2007) Nanotube enhanced photoresponse of carbon modified (CM)-n-TiO_2 for efficient water splitting. Sol Energy Mater Sol Cells 91(10):938–943
117. Momeni MM, Ghayeb Y, Ghonchegi Z (2015) Visible light activity of sulfur-doped TiO_2 nanostructure photoelectrodes prepared by single-step electrochemical anodizing process. J Solid State Electrochem 19(5):1359–1366
118. Siuzdak K, Szkoda M, Sawczak M et al (2015) Enhanced photoelectrochemical and photocatalytic performance of iodine-doped titania nanotube arrays. RSC Adv 5(62):50379–50391
119. Mollavali M, Falamaki C, Rohani S (2015) Preparation of multiple-doped TiO_2 nanotube arrays with nitrogen, carbon and nickel with enhanced visible light photoelectrochemical activity via single-step anodization. Int J Hydrog Energy 40(36):12239–12252
120. Choi W, Termin A, Hoffmann MR (1994) The role of metal ion dopants in quantum-sized TiO_2: correlation between photoreactivity and charge carrier recombination dynamics. J Phys Chem 98(51):13669–13679
121. Macak JM, Ghicov A, Hahn R et al (2006) Photoelectrochemical properties of N-doped self-organized titania nanotube layers with different thicknesses. J Mater Res 21(11):2824–2828
122. Ghicov A, Macak JM, Tsuchiya H et al (2006) Ion implantation and annealing for an efficient N-doping of TiO2 nanotubes. Nano Lett 6(5):1080–1082
123. Chai Y, Lin L, Zhang K et al (2014) Efficient visible-light photocatalysts from Gd–La codoped TiO_2 nanotubes. Ceram Int 40(2):2691–2696
124. Kang Y, Zhao J, Tao J et al (2008) Electrochemical deposition of co nanowire arrays into self-organized titania nanotubes. Appl Surf Sci 254(13): 3935–3938
125. Khakpash N, Simchi A, Jafari T (2012) Adsorption and solar light activity of transition-metal doped TiO2 nanoparticles as semiconductor photocatalyst. J Mater Sci Mater Electron 23(3):659–667
126. Zhao L, Wang H, Huo K et al (2011) Antibacterial nano-structured titania coating incorporated with silver nanoparticles. Biomaterials 32(24):5706–5716
127. Paramasivam I, Macak JM, Ghicov A et al (2007) Enhanced photochromism of Ag loaded self-organized TiO_2 nanotube layers. Chem Phys Lett 445(4): 233–237
128. Chen C, Wang N, Zhou P et al (2016) Electrochemically reduced graphene oxide on well-aligned titanium dioxide nanotube arrays for betavoltaic enhancement. ACS Appl Mater Interfaces 8(37):24638–24644
129. Chen S, Paulose M, Ruan C et al (2006) Electrochemically synthesized CdS nanoparticle-modified TiO_2 nanotube-array photoelectrodes: preparation, characterization, and application to photoelectrochemical cells. J Photochem Photobiol A Chem 177(2):177–184
130. Yang L, Luo S, Liu R et al (2010) Fabrication of CdSe nanoparticles sensitized long TiO_2 nanotube arrays for photocatalytic degradation of anthracene-9-carbonxylic acid under green monochromatic light. J Phys Chem C 114(11): 4783–4789
131. Hou Y, Li X, Zhao Q et al (2010) Electrochemically assisted photocatalytic degradation of 4-chlorophenol by ZnFe2O4–modified TiO_2 nanotube array electrode under visible light irradiation. Environmental science & technology 44(13):5098–5103
132. Sun WT, Yu Y, Pan HY et al (2008) CdS quantum dots sensitized TiO_2 nanotube-array photoelectrodes. J Am Chem Soc 130(4):1124–1125
133. Benoit A, Paramasivam I, Nah YC et al (2009) Decoration of TiO_2 nanotube layers with WO_3 nanocrystals for high-electrochromic activity. Electrochem Commun 11(4):728–732
134. Roy P, Kim D, Paramasivam I et al (2009) Improved efficiency of TiO_2 nanotubes in dye sensitized solar cells by decoration with TiO_2 nanoparticles. Electrochem Commun 11(5):1001–1004
135. Roy P, Albu SP, Schmuki P (2010) TiO_2 nanotubes in dye-sensitized solar cells: higher efficiencies by well-defined tube tops. Electrochem Commun 12(7):949–951
136. Assaud L, Brazeau N, Barr MKS et al (2015) Atomic layer deposition of Pd nanoparticles on TiO2 nanotubes for ethanol electrooxidation: synthesis and electrochemical properties. ACS Appl Mater Interfaces 7(44):24533–24542
137. Ng S, Kuberský P, Krbal M et al (2018) ZnO coated anodic 1D TiO2 nanotube layers: efficient photo-electrochemical and gas sensing heterojunction. Adv Eng Mater 20(2):1700589
138. Zazpe R, Knaut M, Sopha H et al (2016) Atomic layer deposition for coating of high aspect ratio TiO2 nanotube layers. Langmuir 32(41):10551–10558
139. Krbal M, Prikryl J, Zazpe R et al (2017) CdS-coated TiO 2 nanotube layers: downscaling tube diameter towards efficient heterostructured photoelectrochemical conversion. Nanoscale 9(23):7755–7759
140. Sopha H, Krbal M, Ng S et al (2017) Highly efficient photoelectrochemical and photocatalytic anodic TiO2 nanotube layers with additional TiO2 coating. Applied Materials Today 9:104–110
141. Jang NS, Kim MS, Kim SH et al (2014) Direct growth of titania nanotubes on plastic substrates and their application to flexible gas sensors. Sensors Actuators B Chem 199:361–368
142. Enachi M, Lupan O, Braniste T et al (2015) Integration of individual TiO_2 nanotube on the chip: nanodevice for hydrogen sensing. physica status solidi (RRL)-Rapid Research Letters 9(3):171–174
143. Chen B, Hou J, Lu K (2013) Formation mechanism of TiO_2 nanotubes and their applications in photoelectrochemical water splitting and supercapacitors. Langmuir 29(19):5911–5919
144. Snaith H, Docampo P (2014) Solid state dye-sensitized solar cell—encyclopedia of applied electrochemistry. Springer, New York, pp 2029–2040
145. Mor GK, Shankar K, Paulose M et al (2007) High efficiency double heterojunction polymer photovoltaic cells using highly ordered TiO_2 nanotube arrays. Appl Phys Lett 91(15):152111
146. Varghese OK, Paulose M, Grimes CA (2009) Long vertically aligned titania nanotubes on transparent conducting oxide for highly efficient solar cells. Nat Nanotechnol 4(9):592–597
147. Varghese OK, Paulose M, LaTempa TJ et al (2009) High-rate solar photocatalytic conversion of CO_2 and water vapor to hydrocarbon fuels. Nano Lett 9(2):731–737
148. Nakata K, Fujishima A (2012) TiO 2 photocatalysis: design and applications. J Photochem Photobiol C: Photochem Rev 13(3):169–189
149. Mohamed AM, Aljaber AS, AlQaradawi SY et al (2015) TiO_2 nanotubes with ultrathin walls for enhanced water splitting. Chem Commun 51(63):12617–12620
150. Chen D, Zhang H, Li X et al (2010) Biofunctional titania nanotubes for visible-light-activated photoelectrochemical biosensing. Anal Chem 82(6): 2253–2261
151. Popat KC, Eltgroth M, LaTempa TJ et al (2007) Decreased Staphylococcus epidermis adhesion and increased osteoblast functionality on antibiotic-loaded titania nanotubes. Biomaterials 28(32):4880–4888
152. Gulati K, Ramakrishnan S, Aw MS et al (2012) Biocompatible polymer coating of titania nanotube arrays for improved drug elution and osteoblast adhesion. Acta Biomater 8(1):449–456
153. Park J, Bauer S, Schlegel KA et al (2009) TiO_2 nanotube surfaces: 15 nm—an optimal length scale of surface topography for cell adhesion and differentiation. Small 5(6):666–671
154. Popat KC, Leoni L, Grimes CA et al (2007) Influence of engineered titania nanotubular surfaces on bone cells. Biomaterials 28(21):3188–3197
155. Vasilev K, Poh Z, Kant K et al (2010) Tailoring the surface functionalities of titania nanotube arrays. Biomaterials 31(3):532–540
156. Mei S, Wang H, Wang W et al (2014) Antibacterial effects and biocompatibility of titanium surfaces with graded silver incorporation in titania nanotubes. Biomaterials 35(14):4255–4265
157. Bauer S, Park J, Faltenbacher J et al (2009) Size selective behavior of mesenchymal stem cells on ZrO_2 and TiO_2 nanotube arrays. Integr Biol 1(8–9):525–532
158. Bauer S, Park J, von der Mark K et al (2008) Improved attachment of mesenchymal stem cells on super-hydrophobic TiO_2 nanotubes. Acta Biomater 4(5):1576–1582
159. Lv L, Liu Y, Zhang P et al (2015) The nanoscale geometry of TiO2 nanotubes influences the osteogenic differentiation of human adipose-derived stem cells by modulating H3K4 trimethylation. Biomaterials 39:193–205
160. Smith BS, Yoriya S, Johnson T et al (2011) Dermal fibroblast and epidermal keratinocyte functionality on titania nanotube arrays. Acta Biomater 7(6): 2686–2696
161. Peng L, Eltgroth ML, LaTempa TJ et al (2009) The effect of TiO2 nanotubes on endothelial function and smooth muscle proliferation. Biomaterials 30(7): 1268–1272
162. Kar A, Raja KS, Misra M (2006) Electrodeposition of hydroxyapatite onto nanotubular TiO_2 for implant applications. Surf Coat Technol 201(6):3723–3731
163. Kodama A, Bauer S, Komatsu A et al (2009) Bioactivation of titanium surfaces using coatings of TiO_2 nanotubes rapidly pre-loaded with synthetic hydroxyapatite. Acta Biomater 5(6):2322–2330
164. Tsuchiya H, Macak JM, Müller L et al (2006) Hydroxyapatite growth on anodic TiO_2 nanotubes. J Biomed Mater Res A 77((3):534–541

165. Oh SH, Finones RR, Daraio C et al (2005) Growth of nano-scale hydroxyapatite using chemically treated titanium oxide nanotubes. Biomaterials 26(24):4938–4943
166. Parcharoen Y, Kajitvichyanukul P, Sirivisoot S et al (2014) Hydroxyapatite electrodeposition on anodized titanium nanotubes for orthopedic applications. Appl Surf Sci 311:54–61
167. von Wilmowsky C, Bauer S, Lutz R et al (2009) In vivo evaluation of anodic TiO_2 nanotubes: an experimental study in the pig. J Biomed Mater Res B Appl Biomater 89((1):165–171
168. Zhao L, Chu PK, Zhang Y et al (2009) Antibacterial coatings on titanium implants. J Biomed Mater Res B Appl Biomater 91(1):470–480
169. Puckett SD, Taylor E, Raimondo T et al (2010) The relationship between the nanostructure of titanium surfaces and bacterial attachment. Biomaterials 31(4):706–713
170. Ercan B, Taylor E, Alpaslan E et al (2011) Diameter of titanium nanotubes influences anti-bacterial efficacy. Nanotechnology 22(29):295102
171. Bauer S, Park J, Pittrof A et al (2011) Covalent functionalization of TiO_2 nanotube arrays with EGF and BMP-2 for modified behavior towards mesenchymal stem cells. Integr Biol 3(9):927–936
172. Feng W, Geng Z, Li Z et al (2016) Controlled release behaviour and antibacterial effects of antibiotic-loaded titania nanotubes. Mater Sci Eng C 62:105–112
173. Zhang H, Sun Y, Tian A et al (2013) Improved antibacterial activity and biocompatibility on vancomycin-loaded TiO_2 nanotubes: in vivo and in vitro studies. Int J Nanomedicine 8:4379
174. Ma M, Kazemzadeh-Narbat M, Hui Y et al (2012) Local delivery of antimicrobial peptides using self-organized TiO_2 nanotube arrays for peri-implant infections. J Biomed Mater Res A 100((2):278–285
175. Aw MS, Kurian M, Losic D (2014) Non-eroding drug-releasing implants with ordered nanoporous and nanotubular structures: concepts for controlling drug release. Biomaterials Science 2(1):10–34
176. Popat KC, Eltgroth M, LaTempa TJ et al (2007) Titania nanotubes: a novel platform for drug-eluting coatings for medical implants. Small 3(11):1878–1881
177. Hu Y, Cai K, Luo Z et al (2012) TiO_2 nanotubes as drug nanoreservoirs for the regulation of mobility and differentiation of mesenchymal stem cells. Acta Biomater 8(1):439–448
178. Lai M, Jin Z, Tang Q, et al. Sustained release of melatonin from TiO_2 nanotubes for modulating osteogenic differentiation of mesenchymal stem cells in vitro. J Biomater Sci Polym Ed. 2017;1–29.
179. Lee YH, Bhattarai G, Park IS et al (2013) Bone regeneration around N-acetyl cysteine-loaded nanotube titanium dental implant in rat mandible. Biomaterials 34(38):10199–10208
180. Cheng H, Li Y, Huo K et al (2014) Long-lasting in vivo and in vitro antibacterial ability of nanostructured titania coating incorporated with silver nanoparticles. J Biomed Mater Res A 102(10):3488–3499
181. Huo K, Zhang X, Wang H et al (2013) Osteogenic activity and antibacterial effects on titanium surfaces modified with Zn-incorporated nanotube arrays. Biomaterials 34(13):3467–3478
182. Zhao L, Wang H, Huo K et al (2013) The osteogenic activity of strontium loaded titania nanotube arrays on titanium substrates. Biomaterials 34(1):19–29
183. Zhang X, Wu H, Geng Z et al (2014) Microstructure and cytotoxicity evaluation of duplex-treated silver-containing antibacterial TiO_2 coatings. Mater Sci Eng C 45:402–410
184. Gao A, Hang R, Huang X et al (2014) The effects of titania nanotubes with embedded silver oxide nanoparticles on bacteria and osteoblasts. Biomaterials 35(13):4223–4235
185. Hu H, Zhang W, Qiao Y et al (2012) Antibacterial activity and increased bone marrow stem cell functions of Zn-incorporated TiO_2 coatings on titanium. Acta Biomater 8(2):904–915
186. Velard F, Laurent-Maquin D, Braux J et al (2010) The effect of zinc on hydroxyapatite-mediated activation of human polymorphonuclear neutrophils and bone implant-associated acute inflammation. Biomaterials 31(8):2001–2009
187. Yusa K, Yamamoto O, Fukuda M et al (2011) In vitro prominent bone regeneration by release zinc ion from Zn-modified implant. Biochem Biophys Res Commun 412(2):273–278